



**HAL**  
open science

## A new agro-hydrological catchment model to assess the cumulative impact of small reservoirs

Nicolas Lebon, Cécile Dagès, Delphine Leenhardt, Jérôme Molenat

### ► To cite this version:

Nicolas Lebon, Cécile Dagès, Delphine Leenhardt, Jérôme Molenat. A new agro-hydrological catchment model to assess the cumulative impact of small reservoirs. *Environmental Modelling and Software*, 2022, 153, pp.105409. 10.1016/j.envsoft.2022.105409 . hal-03673105

**HAL Id: hal-03673105**

**<https://hal.inrae.fr/hal-03673105v1>**

Submitted on 22 Jul 2024

**HAL** is a multi-disciplinary open access archive for the deposit and dissemination of scientific research documents, whether they are published or not. The documents may come from teaching and research institutions in France or abroad, or from public or private research centers.

L'archive ouverte pluridisciplinaire **HAL**, est destinée au dépôt et à la diffusion de documents scientifiques de niveau recherche, publiés ou non, émanant des établissements d'enseignement et de recherche français ou étrangers, des laboratoires publics ou privés.



Distributed under a Creative Commons Attribution - NonCommercial 4.0 International License

# 1 **A new agro-hydrological catchment model to assess the cumulative impact** 2 **of small reservoirs**

3 Nicolas Lebon<sup>1,2</sup>, Cécile Dagès<sup>1</sup>, Delphine Burger-Leenhardt<sup>2</sup>, Jérôme Molénat<sup>1</sup>

4 <sup>1</sup>LISAH, Univ Montpellier, INRAE, Institut Agro, IRD, 2 Place Pierre Viala, 34000 Montpellier,  
5 France

6 <sup>2</sup>AGIR, Toulouse University, INRAE, INPT, INP-EI PURPAN, 24 Chemin de Borde-Rouge, 31326  
7 Castanet Tolosan Cedex, France

8 Correspondence: Jérôme Molénat, LISAH, Univ Montpellier, INRAE, Institut Agro, IRD, 2 Place  
9 Pierre Viala, 34000 Montpellier, France (email: [jerome.molenat@inrae.fr](mailto:jerome.molenat@inrae.fr); phone: +33 6 87 38 37 08)

10

## 11 **Highlights:**

- 12 ● We present an agro-hydrological catchment model considering small reservoirs
- 13 ● Catchment elements (reservoir, plot, stream reach, etc.) are explicitly represented
- 14 ● The model satisfactorily simulates hydrological and agricultural variables and fluxes
- 15 ● Local and cumulative impacts of small reservoirs are simulated
- 16 ● One of the goals of the model is to gain insight into the causes of the impacts

17

18 **Abstract:** Small-reservoir development is a challenging issue in agricultural catchments facing water  
19 scarcity. An integrated, new and original agro-hydrological model considering small reservoirs,  
20 MHYDAS-Small-Reservoirs, is presented. The model explicitly represents relevant spatial scales  
21 (plot, small-reservoir, stream reach, groundwater, and catchment scales) and the agronomic and  
22 hydrological links between these scales at which agriculture-hydrology interactions occur. After  
23 numerical verification, the model is evaluated by applying it to a 19-km<sup>2</sup> catchment. The model  
24 satisfactorily simulates the annual stream runoff (within 6%) and daily stream runoff (Nash  
25 efficiency=0.47) but tends to overestimate the crop yield (+21%). Simulations, one under actual basin

26 conditions and one under virtual conditions, were carried out. This highlighted the potential of the  
27 model to predict the local and cumulative impacts of small reservoirs. Hence, MHYDAS-Small-  
28 Reservoirs is a promising model for land use planning and water management of agricultural  
29 catchments containing small reservoirs.

30

31

32 **Keywords:** small reservoirs, crop, plot, farmer decisions, agricultural water management

33

## 34 **Introduction**

35 The frequency of droughts has been increasing worldwide in many arid and semi-arid regions (East  
36 Asia, Africa, Australia, and the Mediterranean basin) and temperate regions, such as Western Europe  
37 (Spinoni et al., 2013). Drought occurrences may increase in the future due to climate change (Sheffield  
38 and Wood, 2008) and anthropogenic pressures on water resources (Vörösmarty et al., 2000). Droughts  
39 induce severe consequences notably on hydrology and agriculture (Van Loon, 2015, Malakoff and  
40 Sugden, 2020). In agricultural catchments, small reservoirs are considered by water managers and  
41 farmers as a potential way to adapt agricultural practices to drought occurrences (e.g., Rodrigues et al.,  
42 2012; Malveira et al., 2012; Albergel et al., 2005; Essegbey et al., 2012). Previous global studies have  
43 shown the often-overlooked potential of small water storage to increase water and food security. Small  
44 water storage or a soft-path approach would avoid the construction of large, capital intensive, and  
45 environmentally damaging water infrastructure. Previous studies estimated that irrigation with small  
46 reservoirs can globally feed an additional 800 million people under current climate conditions (Rosa et  
47 al., 2020a) and an additional 300 million people under a 3°C warmer climate (Rosa et al., 2020b).  
48 Most of these studies are global and cannot account for many local site-specific variables.

49 Small reservoirs are reservoirs whose storage capacity does not exceed  $10^6$  m<sup>3</sup> (Habets et al., 2018).  
50 By intercepting and storing surface, subsurface and stream runoff during high-flow periods, they

51 constitute an alternative water resource for crop irrigation purposes during drought periods. As a  
52 consequence, the number of small reservoirs has multiplied in recent decades in many regions  
53 worldwide, and their spatial density may exceed 5 small reservoirs per km<sup>2</sup> (Habets et al., 2018).  
54 However, the increase in small reservoirs may impose antagonistic impacts. As a positive effect, small  
55 reservoirs represent an alternative resource required to maintain crop yields (Biemans et al., 2011;  
56 Wisser et al., 2010). As a negative effect, each small reservoir may have a local hydrological effect on  
57 its nearby environment, such as by modifying the groundwater-surface exchanges or reducing the  
58 stream flow. The reservoirs taken as a whole (the reservoir network) may also induce a cumulative  
59 effect. Hydrological modifications, especially local modifications, may induce ecological,  
60 biogeochemical and geomorphological disturbances in catchments and the ecosystems they support  
61 (Habets et al., 2018).

62 Small reservoirs in an agricultural catchment enhance the interactions between hydrology and  
63 agriculture, particularly through crop water needs and farmers' decisions on crop management and  
64 water withdrawals for irrigation (Figure 1). The elucidation and prediction of the hydrological and  
65 agricultural impacts of small reservoirs require the articulation of the different spatial scales involved  
66 in these interactions:

- 67 i. the agricultural plot, where farmers decide cropping practices, where crop growth occurs and  
68 where water is partitioned between evaporation, transpiration, runoff and infiltration
- 69 ii. the small reservoir, which, on the one hand, is related to its upstream hydrological drained  
70 area and downstream catchment area and, on the other hand, to each irrigated plot
- 71 iii. the catchment, which integrates hydrological effects, especially those on stream runoff and  
72 groundwater.

73 These different scales are linked by hydrological processes (surface runoff, stream runoff,  
74 groundwater recharge, etc.) and crop and agricultural water management operations (water withdrawal  
75 operations from reservoirs and irrigation applications).

76 Numerical modelling is a widely adopted approach to better understand and predict small-reservoir  
77 impacts. Most of the models dedicated to this aim are based on hydrological catchment models.  
78 Among these hydrological models, few explicitly consider the plot scale at which management  
79 operations are conducted. The spatial representation of reservoirs can be explicit (Deitch et al., 2013;  
80 Nathan et al., 2005), statistical (e.g., Çetin et al., 2009; Güntner et al., 2004; Nathan et al., 2005;  
81 Zhang et al., 2012) or global (e.g., Habets et al., 2014; Perrin et al., 2012; Tarboton and Schulze,  
82 1991). The explicit spatial representation has the advantage of simulating both local and cumulative  
83 hydrological impacts of the reservoir networks (Deitch et al., 2013; Nathan et al., 2005). Regarding the  
84 representation of crop growth, very few models couple crop and hydrological models (e.g., Neitsch et  
85 al., 2011; Therond et al., 2014). Most models simply represent crop growth through functional  
86 parameters (e.g., leaf area and crop development coefficient) or forcing variables (transpiration  
87 fluxes), while other models neglect this aspect. The interaction between crop growth and hydrological  
88 processes is thus not considered. Water withdrawal from reservoirs and the irrigation amount applied  
89 to crops can be modelled depending on both crop water requirements and water availability (Murgue  
90 et al., 2014; Neitsch et al., 2011). However, certain models consider constant irrigation amounts over  
91 given periods (e.g., Hughes and Mantel, 2010), while others do not consider crop irrigation (e.g.,  
92 Rousseau et al., 2013). With the exception of very few catchment models (e.g., Therond et al., 2014),  
93 farmer decisions on crop and agricultural water management are not represented in catchment models  
94 dedicated to agricultural catchments containing small reservoirs. Finally, to our knowledge, very few,  
95 if any, of these models simultaneously consider the various spatial scales (plot, reservoir, and  
96 catchment), the water dynamics in small reservoirs in relation to water withdrawals and the agronomic  
97 and hydrological links between these scales at which agriculture-hydrology interactions occur.

98 We developed a new distributed agro-hydrological model named MHYDAS-Small-Reservoirs. This  
99 model is designed for agricultural catchments containing small reservoirs dedicated to irrigation. It  
100 simulates the interactions between the hydrological behaviour of the catchment, crop growth and  
101 farmer decisions related to the management of crops and reservoirs. MHYDAS-Small-Reservoirs is  
102 based on the coupling of three already proven models: i) the catchment-scale distributed MHYDAS

103 hydrological model (Moussa et al., 2002), ii) the plot-scale crop model AqYield (Constantin et al.,  
104 2015) that includes yield calculation and iii) a plot and reservoir-scale farmer's decision model  
105 (Murgue et al. 2014), without any name, that represents the farmer decisions related to crop and water  
106 reservoir management. The latter two have already been used in a water management model, Maelia,  
107 (Therond et al., 2014), which has been applied to water resource catchments of 1000-10,000 km<sup>2</sup> with  
108 reservoirs dedicated to irrigation (e.g., Aveyron catchment in France, Allain et al., 2018). The spatial  
109 representation used for MHYDAS-Small-Reservoirs combines landscape objects (e.g., plot, reservoir)  
110 at the catchment scale and is based on that of MHYDAS, fully described in Lagacherie et al (2010).  
111 This representation proves to be particularly effective for simulating surface hydrology (e.g., Hallema  
112 et al., ), erosion (e.g., Gumière et al., 2011) or pesticide transfer (e.g., Bouvet et al., 2010) in small to  
113 medium agricultural catchments. The main novelty of this model is thus the explicit representation of  
114 the relevant spatial scales (plot, reservoir, and catchment) and the links between these scales involved  
115 in hydrology-agriculture interactions. MHYDAS-Small-Reservoirs is intended to be used in  
116 catchments of 10-100 km<sup>2</sup> to understand and estimate the local and cumulative effects of small  
117 reservoirs on the hydrology of catchments, especially stream runoff, and on crop production.

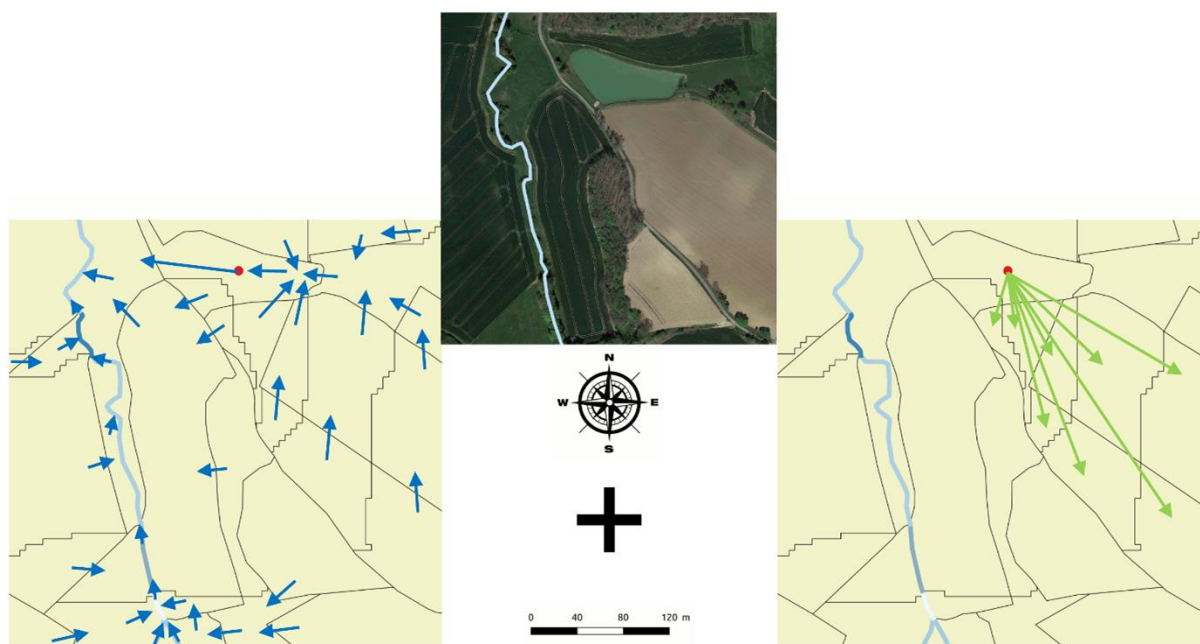
118 The objective of this paper is fourfold. First, it describes the principles of MHYDAS-Small-Reservoirs  
119 in terms of catchment spatial segmentation and the modelling of hydrological processes, crop growth  
120 and farmer management practices of crops and reservoirs. Second, it demonstrates the numerical and  
121 computing consistency of the model. Third, it demonstrates the capacity of the model to represent the  
122 hydrological and agricultural functioning of an agricultural catchment containing small reservoirs, via  
123 an application to a real case study (the Gélon catchment, France). Fourth, it investigates the feasibility  
124 of model application in the examination of the hydrological and agricultural impacts of catchment  
125 situations in terms of the density of reservoirs dedicated to irrigation.

## 126 **1. Model description**

## 127 1.1 Spatial segmentation

128 The catchment is segmented in spatially homogeneous units according to the principles adopted for  
 129 MHYDAS model representation (Moussa et al., 2002) and fully described and discussed in Lagacherie  
 130 et al. (2010), as shown in Figure 1.

131



132

133 **Figure 1:** Spatial segmentation of the MHYDAS-Small-Reservoirs model. Top: satellite view of a  
 134 catchment area including one non-connected reservoir used for irrigation, agricultural plots and  
 135 hydrographic network (blue line). Bottom: spatial segmentation in MHYDAS-Small-Reservoirs of this  
 136 catchment area. The polygons delimited by the black lines are entire or partial plots called surface  
 137 units (SUs). The blue lines represent the reach segment units (RSs). The red dot indicates a non-  
 138 connected reservoir unit (RE). The water transfer between plots is indicated by arrows. Water transfer  
 139 is the result of hydrological processes (the hydrological links are marked in blue in the left map) or  
 140 water withdrawal to irrigate crops (the agronomical links are marked in green in the right map).

141 Four spatial unit types, corresponding to the physical elements of a catchment, are explicitly  
 142 represented in MHYDAS-Small-Reservoirs (Figure 1):

143 • The surface unit (SU) represents a homogeneous spatial entity in terms of its properties (soil  
144 and land use) corresponding to one sub-part of a real plot with a uniform water flow direction.  
145 Therefore, depending on the topography, a real agricultural or non-agricultural plot may be  
146 represented in the model as a unique SU or several SUs. The SU boundaries are determined by  
147 overlapping three geographical layers: the plot map, the flow direction map derived from the  
148 topography and the soil map (Lagacherie et al., 2010). An agricultural SU is dedicated to crop  
149 cultivation and can be irrigated. Non-agricultural SUs are plots with non-cultivated vegetation, such as  
150 forests, moors or natural pastures, or non-vegetated plots (e.g., urban areas, bare rock areas, and sand  
151 areas).

152 • The water reservoir unit (RE) represents a reservoir that can eventually be used for irrigation.  
153 The RE directly connected upstream to a certain reach of the hydrographic network is hereafter called  
154 a connected RE. This type of RE is filled by surface runoff from upstream SUs, stream runoff from  
155 upstream RSs, and direct rainfall. In some countries, a minimum flow prescribed by environmental  
156 regulations has to be released downstream. The RE not connected upstream to a reach is hereafter  
157 called a non-connected RE. Unlike a connected RE, a non-connected RE is not filled by stream runoff  
158 from upstream RSs, and a minimum flow has not been prescribed to be released downstream.

159 • The groundwater unit (GU) represents a hillslope shallow aquifer characterised by a  
160 subsurface saturated flow following the structure of the hydrological catchment. Each GU is therefore  
161 derived from the topography considered to identify the flow direction. Each GU discharges in a single  
162 specific reach segment (RS).

163 • The reach segment unit (RS) represents a section of the hydrographic network between water  
164 sources, confluence points, and connected RE or SU boundaries. RSs are connected to comprise the  
165 hydrographic network. An RS can be used for irrigation purposes.

166 These four spatial unit types differ in their shape and geometrical properties (Table 1). SUs and GUs  
167 are polygons whose boundaries are fixed based on the topography and anthropogenic discontinuities  
168 (plots, vegetation cover, etc.). RSs are linear elements, while REs are represented by points.



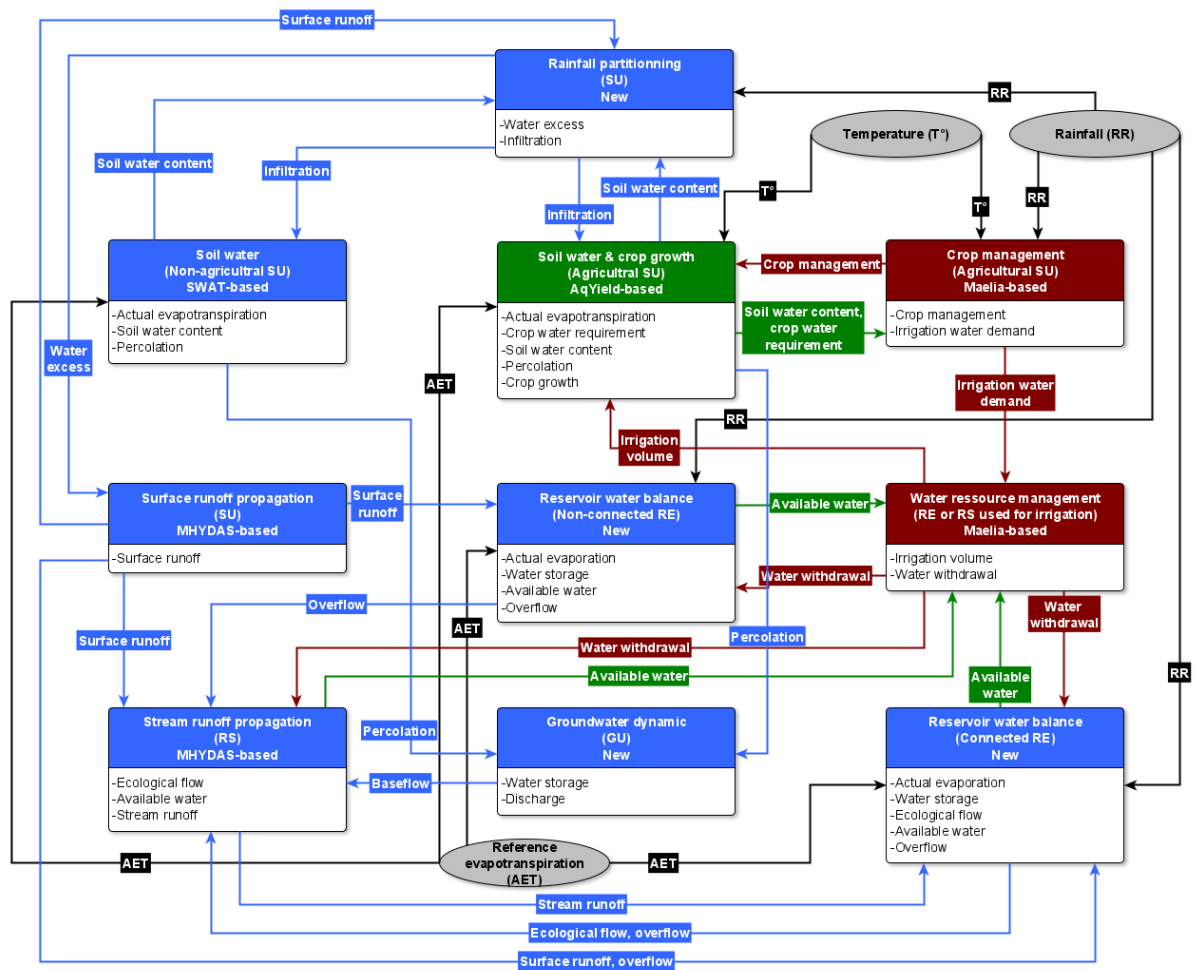
169 **Table 1:** Main geometrical properties of the spatial unit types in MHYDAS-Small-Reservoirs. The  
 170 flow distance between any two units corresponds to the distance between the centroids of these two  
 171 units.

	<b>Surface Unit (SU)</b>	<b>Reservoir Unit (RE)</b>	<b>Reach Segment Unit (RS)</b>	<b>Groundwater Unit (GU)</b>
<b>Geometrical properties</b>	Flow distance (m) Position (x,y,z) Slope (m/m) Area (m <sup>2</sup> )	Position (x,y,z) Volume capacity (m <sup>3</sup> ) Maximum water surface (m <sup>2</sup> ) Volume-to- surface ratio (m <sup>3</sup> /m <sup>2</sup> )	Position (x,y,z) Slope (m/m) Length (m) Width (m) Height (m)	Position (x,y,z) Area (m <sup>2</sup> )

172 These units are linked by two types of relations:

- 173 • Hydrological links correspond to the water flows caused by a hydrological process, such as  
 174 surface runoff, stream runoff, drainage, and groundwater discharge. To establish a hydrological link  
 175 between SUs, REs and RSs, it is assumed that surface water (surface and stream runoff) flows along  
 176 the steepest slope to a downstream spatial unit (RE, RS or SU). Every GU is linked to its upstream  
 177 SUs and downstream RS.
- 178 • Agronomic links correspond to the water transfer from a water resource (RE or RS) to an  
 179 irrigated SU. A water resource can be linked to one or several SUs.

180 In the three following sections, the hydrological, crop growth and crop and agricultural withdrawal  
 181 management models are described. The equations are shown for the new model developed specifically  
 182 for the MHYDAS-Small-Reservoir model.



183  
 184 **Figure 2:** Diagram of the different components of the MHYDAS-Small-Reservoirs model (coloured  
 185 boxes), simulated flows (black, green, blue or red lines) and state variables (grey circles). The black,  
 186 blue, green and red arrows correspond to the exchanged variables between the model's components  
 187 coloured according to their type of climate forcing variables, hydrological variables, agronomic  
 188 variables and crop and water management variables, respectively. For each model, the simulated flows  
 189 are listed in the corresponding box. The grey circles represent the input variables. The colour of the  
 190 boxes indicates the type of model's component according to whether it is hydrological (blue),  
 191 agronomic (green), or crop and water management (red)

## 192 1.2 Hydrological processes

193 The fluxes and state variables associated with the following hydrological processes are calculated for  
 194 each spatial unit corresponding to one of the physical elements (SU, RS, RE, or GU) and at each time  
 195 step. The time step can range from 1 s to 1 d for all simulated hydrological processes, except for the  
 196 percolation and evapotranspiration of agricultural SUs, which are simulated at a daily time step.

### 197 1.2.1 Water excess, infiltration, percolation and soil water content

198 The water excess is the fraction of the water inputs (i.e., rainfall, irrigation or upstream runoff) that  
 199 does not infiltrate and runs off along the soil surface. Infiltration is the water input fraction infiltrating  
 200 into the soil. The water input distribution between infiltration and water excess is simulated by  
 201 considering the soil infiltration capacity concept. The maximum infiltration rate is equal to the  
 202 infiltration capacity. The soil infiltration capacity varies over time depending on the temporal  
 203 variations in the soil water content. A power law is adopted to relate the soil infiltration capacity and  
 204 soil water content:

$$205 \quad f_p(t_i) = (I_{max} - K_s) * \left( \frac{SW_s - SW(t_i)}{SW_s - SW_r} \right)^\lambda + K_s$$

206

207

Equation 1

208 where  $f_p$  is the soil infiltration capacity (m/s),  $t_i$  is the current time index,  $K_s$  is the mean saturated  
 209 hydraulic conductivity (m/s) over the full soil depth,  $I_{max}$  is the maximum soil infiltration capacity  
 210 (m/s),  $SW_s$  and  $SW_r$  are the soil water storage capacities (m) considering the total soil porosity and the  
 211 water-filled soil porosity at the residual water content, respectively,  $SW$  is the available water storage  
 212 (m) and  $\lambda$  is a shape parameter (-).

213 In the soil, the percolation, evaporation and transpiration are considered the main drivers of the soil  
 214 water dynamics. The soil water dynamics modelling differs between agricultural and non-agricultural  
 215 SUs. In agricultural SUs, the soil is divided in three homogeneous layers, following the AqYield

216 model formalisms (Constantin et al. 2015). The effect of tillage on soil is simulated by decreasing the  
217 water storage capacity of the top soil layer every day after the tillage. The soil water balance is  
218 calculated at a daily time step by simulating the soil water content, crop transpiration, soil evaporation  
219 and percolation. In non-agricultural SUs, Soil and Water Assessment Tool (SWAT) model formalisms  
220 are adopted, with the principle that percolation in soil occurs as soon as the soil water content exceeds  
221 the retention capacity (Neitsch et al., 2011). The soil is divided into several layers for which the water  
222 content is calculated by considering evapotranspiration, infiltration and percolation. These SWAT  
223 formalisms are adapted for use at the sub-daily time scale, as they are not very sensitive to time scale  
224 changes (Brighenti et al., 2019; Maharjan et al., 2013). Regardless of the type of the SU (agricultural  
225 and non-agricultural), the water flows downward from one layer once the soil water content in the  
226 layer reaches the soil water capacity. The simulated percolation flux along the soil base of any SU,  
227 whether agricultural or non-agricultural, contributes to the simulated recharge of the GU connected to  
228 the SU.

### 229 **1.2.2 Surface and stream runoff**

230 Surface and stream runoff are simulated with the diffusive wave equation solved by the Hayami kernel  
231 method assuming a unidirectional flow to represent runoff routing as described by Moussa and  
232 Bocquillon (1996). Surface runoff corresponds to the downslope propagation of the water excess.  
233 Surface runoff flows downstream from an SU to another SU, an RS or an RE, depending on the spatial  
234 segmentation. Stream runoff is simulated at every time step in every RS considering the upstream flow  
235 from any connected SUs, RSs, REs and GUs to the given RS. The simulated stream runoff from an RS  
236 or RE flows into either a downstream RS or downstream RE. Every ~~RS~~ connected RE or RS used for  
237 irrigation is characterised by a user-defined parameter called minimum flow used, denoted  $Q_{\min}$  ( $\text{m}^3 \cdot \text{s}^{-1}$ ),  
238 <sup>1</sup>), to model the withdrawals (see section 1.4.2 Management of the withdrawal from water resources).  
239 The minimum flow is a floor threshold introduced to represent the minimum flow imposed by water  
240 regulation laws to maintain the ecological quality of the stream. Any water withdrawal can be  
241 performed in the stream only if the stream runoff does not fall below this floor threshold.



267 connected RE and iii) the direct rainfall volume. The latter is calculated as the product of the rainfall  
 268 rate and the reservoir maximum water surface. The infiltration through the reservoir bed is not  
 269 considered. Outflows may include i) minimum flow, ii) overflow, iii) evaporation volume and iv)  
 270 water withdrawal for crop irrigation.

271

$$V_{RE}(t_i) = (Q_{REup}(t_i) - Q_{REout}(t_i)) * (t_i - t_{i-1}) + R(t_i) * A_{REmax} - E(t_i) * A_{RE}(t_i) - W(t_i) + V_{RE}(t_{i-1})$$

272

Equation 3

273 where  $V_{RE}$  is the water volume of the reservoir ( $m^3$ );  $t_i$  and  $t_{i-1}$  are the current and previous time  
 274 indexes, respectively;  $Q_{REup}$  is the runoff from the upstream spatial units ( $m^3.s^{-1}$ );  $Q_{REout}$  is the  
 275 discharge released by the reservoir ( $m^3.s^{-1}$ );  $E$  is the evaporation over the time step (m);  $R$  is the  
 276 rainfall over the time step (m);  $A_{REmax}$  and  $A_{RE}$  are the maximum surface area and the water surface  
 277 area of the reservoir, respectively ( $m^2$ ); and  $W$  is the withdrawal volume ( $m^3$ ). Following the  
 278 conclusion of numerous studies about reservoir evaporation (Lowe et al., 2009; McJannet et al., 2013;  
 279 ), the evaporation is assumed to be proportional by a factor  $k$  to the reference evapotranspiration,  $ET_0$ ,  
 280 such as  $E=k.ET_0$ .

281 The released discharge is simulated differently between the non-connected and the connected  
 282 reservoirs. A non-connected reservoir is generally not equipped with a discharge control system and  
 283 releases water only when it is full. Consequently, the released discharge is modelled as the water  
 284 volume,  $V_{REexceed}$ , exceeding the reservoir storage capacity, such as  $Q_{REout}=V_{REexceed}/(t_i-t_{i-1})$ . When the  
 285 water volume is lower than the storage capacity, the released discharge is simulated as zero. Following  
 286 water regulation rules in some countries, a connected reservoir has to be equipped with a control  
 287 system to release a minimum flow, considered an ecological flow. When the upstream runoff to the  
 288 reservoir exceeds the minimum flow, a discharge equivalent to the regulatory minimum flow has to be  
 289 released. When the upstream runoff is lower than the minimum flow, the equivalent of all the

290 upstream runoff has to be released. In accordance to these regulatory and management rules, the  
 291 released discharge for a connected reservoir,  $Q_{REout}$ , is simulated as follows:



292

293

Equation (4)

### 294 **1.3 Crop growth**

295 The crop growth is calculated only in agricultural SUs at daily time steps based on the principles of the  
 296 AqYield crop model (Constantin et al., 2015). Crop growth, both aerial and root, controls crop  
 297 transpiration and crop yield.

298 The crop aerial development is simulated using a crop coefficient representing foliar growth. Crop  
 299 coefficient dynamics are a function of crop transpiration, development stage (phenology), and various  
 300 parameters specific to a given species. Globally, the crop coefficient increases until the flowering  
 301 stage and then declines until the harvesting stage. Crop development stages, particularly the flowering  
 302 and maturity stages, are simulated based on the concept of growing degree days, with threshold values  
 303 of the growing degree days and parameters specific to each species and cultivar precocity class.

304 The actual crop transpiration is calculated with an empirical function of the maximum transpiration  
 305 and soil water available to roots. The maximum transpiration depends on the crop coefficient and  $ET_0$   
 306 minus soil evaporation. The soil water available to roots varies as a function of root growth. Root  
 307 growth depends on the cumulative daily effective temperature, a species root-growth coefficient and a  
 308 reduction coefficient linked to the soil structure.

309 The crop yield is calculated at harvest as a function of the potential yield, locally defined for a species  
 310 or cultivar precocity class, and the water satisfaction index defined as the ratio of the actual crop  
 311 transpiration to the maximum crop transpiration during the cropping season.

## 312 **1.4 Crop and agricultural withdrawal management**

### 313 **1.4.1 Crop management**

314 The model simulates farmer management decisions at daily time steps and for every agricultural SU.  
315 The decisions are related to several practices (tillage, sowing, harvesting and irrigation), but only one  
316 practice, respecting a given priority order, is operated each day. Technical interventions are simulated  
317 over a given user-defined period of the year. Within this window period, the exact dates of technical  
318 operations and amounts of water applied to crops are determined according to decision rules based on  
319 crop growth and development characteristics, soil type and water content, and weather conditions.  
320 These rules, the priority order between practices, and the window period for each practice and crop  
321 may be adjusted to the context via a user-defined set of parameters. The thusly simulated technical  
322 operations modify the other model variables. Tillage operations affect the soil structure and thus the  
323 soil water content capacity. The sowing and harvesting dates determine the start and end, respectively,  
324 of crop cycles. Irrigation decisions trigger water withdrawal operations from REs or RSs and influence  
325 the SU soil water content and thus the crop growth and crop yield. The irrigation demand by the  
326 farmer depends on the crop water requirement according to its development stage but also accounts for  
327 equipment constraints through a minimum delay between two irrigations.

328 Complementary to the presentation of Murgue et al. (2014), [Appendix A](#) details the simulation rules  
329 applied to farmer management decisions.

### 330 **1.4.2 Management of the withdrawal from water resources**

331 Management of water withdrawal for irrigation purposes is modelled at a daily time step for each  
332 water resource dedicated to irrigation, with RS being first withdrawn, then RE. This approach  
333 prioritizes stream water as a resource used for irrigation.

334 The total irrigation water demand on a given resource (RE or RS) is determined as the sum of the daily  
335 farmer's irrigation demand for all irrigable agricultural SUs linked to that resource. If the available  
336 water in the resource is larger than the total irrigation water demand, the water demand is satisfied by



337 the water withdrawal, and the irrigation volume provided to each SU is equal to its demand.  
 338 Otherwise, the withdrawal volume corresponds to the available water volume in the resource, and the  
 339 irrigation volume applied to each  
 340 SU is  $W(t_i) = \min(V_{WR}(t_{i-1}) - V_{WRmin}; \sum_{j=1}^{n_{SU}} IrrDem_j(t_i))$  proportionally  
 341 reduced compared to the  
 342 water demands.

343

344

### Equation 5

345 where  $W$  is the water withdrawal from the resource ( $m^3$ );  $V_{WR}$  is the water volume in the resource ( $m^3$ );  
 346  $V_{WRmin}$  is the minimum water volume ( $m^3$ ) of the resource below which any withdrawal is never  
 347 performed;  $t_i$  and  $t_{i-1}$  are the current and previous time indexes, respectively;  $IrrDem_j$  is the farmer's  
 348 water demand for  $SU_j$  ( $m^3$ ); and  $n_{SU}$  is the number of SU irrigated from the water resource. The  
 349 minimum water volume of the resource,  $V_{WRmin}$ , corresponds to the minimum flow,  $Q_{min}$ , multiplied by  
 350 the daily time step or to a volume threshold,  $V_{REmin}$ , when the water resource is a stream reach (RS) or  
 351 a reservoir, respectively. The volume threshold,  $V_{REmin}$ , is the water volume below which water  
 352 pumping is technically difficult and usually not performed due to high concentrations of sediments in  
 353 the water. Similarly, the available water volume of the resource,  $V_{WR}$ , corresponds to the reservoir  
 354 water volume,  $V_{RE}$ , and to the stream runoff,  $Q_{RS}$ , multiplied by the daily time step when the resource  
 355 is a reservoir and a stream reach, respectively.

## 356 1.5 Computer implementation

357 The MHYDAS-Small-Reservoirs model was developed within the OpenFLUID platform (Fabre et al.,  
 358 2020; Fabre et al., 2010). This platform facilitates model building by sequentially coupling blocks of  
 359 code, called simulators, with each simulator supporting one of the main model functions. The  
 360 OpenFLUID platform achieves the coupling of models via the exchange of simulation variables  
 361 varying both in space and time. The overall structure of the spatial domain is managed using a graph

362 where the nodes are the spatial units (here, SUs, RSs, GUs, and REs) and the edges are these relations  
363 between the above spatial units (hydrological or agronomic links). MHYDAS-Small-Reservoirs  
364 consists of 16 simulators described in [Appendix B](#) and considers a total of 40 variables. All simulators  
365 were written in the C++ language, which allows unit-oriented data entry (Jordan, 1990).

## 366 **1.6 Input and simulated variables, parameters and initial conditions**

367 The input variables are weather variables, namely, rainfall, ET0 and air temperature (Figure 2). The  
368 input variables are spatially distributed. The simulated variables per spatial unit type are shown in  
369 Figure 2. The parameters adopted in the equations and relations implemented in the simulators are  
370 listed in [Appendix C](#). They correspond to either empirical values or functional properties of the spatial  
371 units. They can be either global (i.e., a unique and common value for all the spatial unit types) or  
372 spatially distributed (i.e., each spatial unit has its own value). The initial model conditions include the  
373 soil water content in all agricultural and non-agricultural SUs, the water level in each GU, and the  
374 volume of water stored in each RE, connected or not.

## 375 **2. Materials and methods**

### 376 **2.1 Study area**

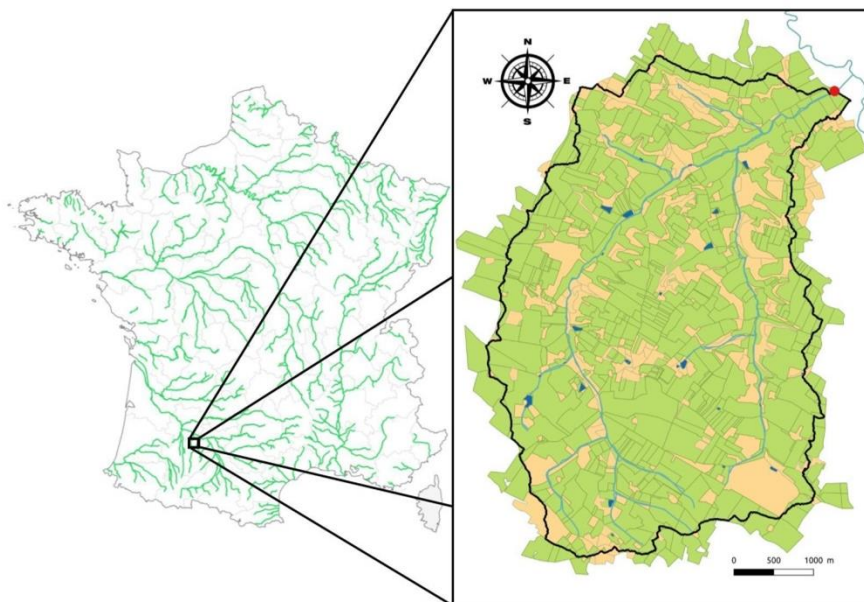
377 The Gélon catchment was chosen for the application of the model, for the hydrologic year 2014-2015,  
378 for which most of the data required for model implementation and evaluation was available, notably  
379 the agricultural plot map.

#### 380 **2.1.1 General characteristics**

381 The Gélon is a 19.8-km<sup>2</sup> catchment belonging to the Arrats catchment, which is a 620 km<sup>2</sup> sub-  
382 catchment of the Garonne River located in southwestern France in the Gers department (Figure 3). The  
383 outlet is located at 43°51'38"N-0°48'07"E. It is a hilly catchment with the elevation ranging from 110  
384 to 193 m above sea level. The soils are mainly composed of alluvial and molassic slope deposits (Party  
385 et al., 2016). The lithology is globally impermeable, without a deep aquifer, which leads to a high  
386 density of the hydrographic network (Cavaillé and BRGM, 1968). The total length of the Gélon stream

387 is 8 km. The oceanic climate of the catchment induces a rainfall of 675 mm, an ET<sub>0</sub> level of 905 mm  
 388 and a temperature of 13.5°C on average over the period from 1989-2016.

389



390

391 **Figure 3:** Location and map of the Gélon catchment. The agricultural and non-agricultural plots in the  
 392 map are marked in green and yellow, respectively. The outlet is indicated by a red dot. The  
 393 hydrographic network and small reservoirs are represented by blue lines and dark blue areas,  
 394 respectively.

395 The Gélon catchment is mostly agricultural. The majority (75%) of the catchment area is devoted to  
 396 agriculture, representing 585 cultivated plots (IGN, 2015). The remaining 25% (244 plots) comprises  
 397 non-cultivated, urbanized or forested areas (MTES, 2012). The whole cultivated area is covered by  
 398 annual field crops, and the main crops are straw cereals (mostly wheat, barley, triticale and oats) and  
 399 sunflower (accounting for 41 % and 33 %, respectively, of the cultivated area in 2015). Maize,  
 400 soybeans, peas, chickpeas, lentils, flax, market gardening (largely garlic, strawberry, butternut and  
 401 onion), sorghum, rapeseed, and temporary and permanent grassland are also cultivated to a lesser  
 402 extent in this region where organic farming is increasingly applied.

403 Most crops are rainfed (sunflower, permanent grassland and vineyard plots), some are systematically  
404 irrigated (mostly maize and soybeans), and others are irrigated only when weather conditions are  
405 particularly dry (straw cereals, temporary grassland, market gardening, rapeseed and orchards). Field  
406 surveys indicate that farmers generally irrigate their fields with an amount of 30 mm, except for  
407 rapeseed, which can be irrigated only once, at the sowing time, with half the amount (i.e., 15 mm).  
408 Irrigation occurs during the cropping season, namely, temporary grasslands are irrigated from April to  
409 mid-May, straw cereals from mid-May to mid-June, maize from mid-May to mid-September, market  
410 gardening from mid-May to mid-October, soybeans and orchards from June to September, and  
411 rapeseed in September.

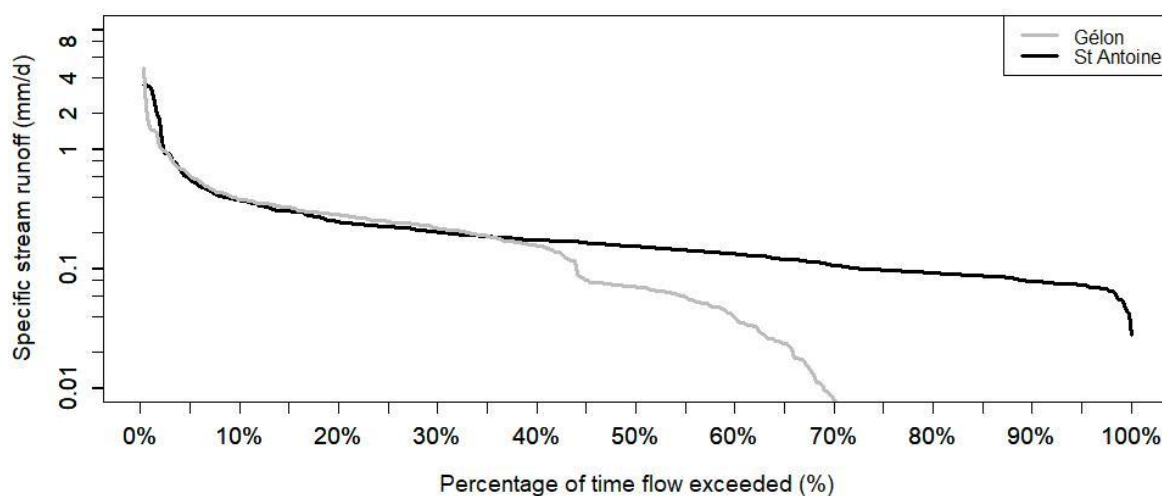
412 The catchment contains 25 water reservoirs of varying capacities (100 to 30,000 m<sup>3</sup>), 13 of which are  
413 used for irrigation, while the remaining 12 reservoirs, often smaller, have no current irrigation use  
414 following the change to non-irrigated crops or following the purchase of the land by private  
415 individuals who are not farmers. The 13 reservoirs are the only resource for irrigation water, i.e., in  
416 this catchment, no water is withdrawn from the river. There are no channel networks: the water is  
417 directly pumped from the reservoirs and distributed to the fields under pressure. Overall, 19 % of the  
418 agricultural area is irrigated, mainly by aspersion using 25-m travelling guns. The limited availability  
419 of irrigation equipment, the time required to install the equipment and the limited flow rate of the  
420 equipment result in a delay between two irrigations of 6 or 7 days depending on the crop.

### 421 **2.1.2 Weather, pedological, agricultural and hydrological data**

422 The weather variables were retrieved from the SAFRAN database of MétéoFrance (Durand et al.,  
423 1993), namely, the hourly rainfall and air temperature and daily ET<sub>0</sub> calculated according to Penman's  
424 formula, at an 8 km x 8 km resolution. The map of the agricultural plots includes the land use at the  
425 field plot level and is available on a yearly basis from the French Land Parcel Identification System  
426 (IGN, 2015). Crop yield data are only available at the Gers department level (6,200 km<sup>2</sup>) from data  
427 collected from agricultural cooperatives by public authorities (DRAAF Occitanie, 2020). No database  
428 provides information about the agricultural practices in the Gélon catchment, but specific surveys offer

429 insights on the irrigation practices in the Gélon and Arrats catchments. The soil data were provided  
 430 by the Référentiel Régional Pédologique, a French soil database (Party et al., 2016).

431 Stream discharge data at the Gélon outlet have only been available since 14/09/2018. We thus  
 432 estimated the 2014-2015 discharge from the daily specific stream runoff data recorded at the closest  
 433 station of the French station hydrometric network, assuming that both specific stream runoffs were  
 434 equal. This assumption was carefully verified over the period 14/09/2018 to 13/09/2019 at a daily time  
 435 step during which the discharge at both catchment outlets was monitored. The similarity was very high  
 436 for 47% of stream runoff (i.e., between 0.086 and 1.0 mm/d) encountered in the Gélon catchment, with  
 437 an  $r^2$  value of 0.68 considering linear regression, an  $NSE_Q$  value of 0.53 and an  $NSE_{\text{sqrt}}$  value of 0.71  
 438 (Figure 4). The similarity was low for extreme stream runoff, lower than 0.086 mm/d (an  $r^2$  value of  
 439 0.02) or higher than 1.0 mm/d (an  $r^2$  value of 0.11).



440

441 **Figure 4:** Flow duration curves for the Gélon and St Antoine stream runoff.

## 442 2.2 Model implementation

### 443 2.2.1 Spatial segmentation

444 Several geographic data sources (Table 2) were adopted to determine and characterise the geometrical  
 445 properties of all spatial units of the Gélon catchment, resulting in 25 REs, 17 GUs, 365 RSs and 2402  
 446 SUs, 1666 of which are agricultural SUs.

447 **Table 2:** Sources of data considered for the segmentation of the Gélon catchment.

Data type	Data source	Spatial resolution
Topography	Digital elevation model (DEM) RGE ALTI 5 m (IGN, 2017)	5 m
Hydrographic network	BD Carthage (Agence de l'Eau et al., 2014)	10 m
Reservoir location and characteristics	Aerial view analysis (IGN, 2016) and in situ surveys	reservoir resolution
Map of the agricultural plots	Land Parcel Identification System (IGN, 2015)	plot resolution
Map of the non-agricultural plots	Land use inventory (MTES, 2012)	plot resolution

### 448 2.2.2 Parametrisation

449 As far as possible, the parameters corresponding to the functional properties ([Appendix C](#)) were  
 450 determined from existing databases, measurements and in situ observations or retrieved from the  
 451 literature.

452 Values of crop growth parameters were fixed based on previous studies. Indeed, these parameters were  
 453 determined previously for several field crops in southwestern France and then validated for three  
 454 rainfed and irrigated spring crops (sunflower, maize, and sorghum) (Constantin et al., 2015), for wheat

455 on 14 experimental sites in France and for rotations on two sites in southwestern France (Tribouillois  
456 et al., 2018). We grouped crops into classes to limit the number of crop parameter sets, especially for  
457 minority crops. For example, the soybean class includes soybeans as the main crop but also peas,  
458 chickpeas, flax and lentils as minority crops. The soil texture and soil depth also used in the crop  
459 growth model are parameters derived from the French soil database (Référentiel Régional  
460 Pédologique, Party et al., 2016) by considering the dominant soil type in each SU. The soils of the  
461 agricultural SU show low variability (all clay-loam soils) and all belong to a single soil class. In  
462 addition, the three shape parameters of the SU infiltration capacity curve (Equation 1) not defined in  
463 the AqYield database, namely,  $I_{max}$ ,  $K_s$  and  $\alpha$ , were adjusted as detailed below. Two of the four  
464 parameters of the GU storage-discharge function were defined based on an analysis of Gélon outflow  
465 discharges during recession periods, while the other two, namely, parameters a and b of Equation 2,  
466 were fitted. A simple calibration of the outflow at the outlet of the Gélon was performed by  
467 considering 3 values for each of the 5 parameters to be fitted and by varying them one at a time. Thus,  
468 only 243 sets of parameters were then tested. The three values were chosen to explore a realistic range  
469 of variation by selecting the minimum and maximum values found in the literature and their arithmetic  
470 mean. The extreme values for the parameters of the SU infiltration curve were defined according to  
471 Mishra et al. (2003), Fernández-Pato et al. (2016), Party et al. (2016) and those for the GU storage-  
472 discharge function from Kirchner (2009).

473

### 474 **2.2.3 Time step of the simulation**

475 An hourly simulation time step was adopted for all the hydrological processes (blue boxes, Figure 2),  
476 except for those processes for which the formalism required a daily time step, as indicated in Section  
477 1, namely, the water balance of agricultural plots as well as crop growth processes, and crop and  
478 agricultural water management operations (red and green boxes, Figure 2).

#### 479 **2.2.4 Climate input variables and initial conditions**

480 Climate input variables, namely, rainfall, ET0 and air temperature were considered spatially uniform  
481 in the application of the model to the Gélon catchment. Due to the lack of data, all the initial  
482 conditions were set using a warm-up approach, consisting of a simulation over a period long enough to  
483 reach equilibrium (Kollet and Maxwell, 2008). In this study, we adopted the recursive simulation  
484 approach described by Ajami et al. (2014): the previous hydrological year from 2013-2014 was  
485 repeated 25 times with constant crop rotations. We verified that the equilibrium state was reached after  
486 these 25 year-long simulations by determining whether the annual simulated variations in water  
487 storage at a one-year interval were lower than 1% in 95% of the units of each type. This warm-up  
488 process was initiated considering a full saturation of the catchment, including a complete filling of the  
489 reservoirs to limit the spin-up time (Rahman et al., 2016).

### 490 **2.3 Model verification**

491 To verify the model, we considered virtual and real catchments and monitored i) each simulator, ii) the  
492 model determinism and iii) the conservation of water volumes. Furthermore, the computation time was  
493 also analysed.

#### 494 **2.3.1 Simulator testing**

495 For each simulator, the agreement between the computer code and conceptual model was verified  
496 using simple test cases. The verifications were based on a comparison of the simulated and expected  
497 values of the variables, with the latter obtained from either algebraic equations or reference  
498 simulations. These tests also allowed us to evaluate the hydrological and agronomic links between all  
499 the units.

500 As an example, the combined testing of the irrigation decision and application simulators (Appendix  
501 C) allowed us to simultaneously verify the following:

- 502 • the identification of all the RE or RS dedicated to irrigation and the links between that water  
503 resource and the irrigable SUs,



- 504 • the consistency between the available water volume, water withdrawal volume, irrigation  
505 water demand and irrigation amount provided to crops, and
- 506 • the absence of withdrawal from a water resource not dedicated to irrigation.

### 507 **2.3.2 Model determinism**

508 Model determinism is guaranteed when identical simulations, repeated in the same computing  
509 environment with unchanged parameterizations, initial conditions and boundary conditions, result in  
510 exactly the same simulated values. A numerical test was performed on a sub-catchment of the Gélon  
511 catchment, modelled with 341 SUs, 112 RSs, 69 GUs and 13 REs, with one of the latter being  
512 dedicated to irrigation. The test was executed by repeating the same 5-year simulation 1,000 times,  
513 and we assessed whether the water volumes in the GUs, REs, and SUs and water fluxes in the SUs and  
514 RSs remained unchanged across the whole catchment.

### 515 **2.3.3 Water volume conservation**

516 Water volume conservation is an important criterion in hydrological model verification. We monitored  
517 the water volume conservation in MHYDAS-Small-Reservoirs at the daily resolution considering the  
518 whole catchment. In the case of perfect water volume conservation, the total volume of all simulated  
519 outflows from the catchment equals the total volume corresponding to the variation in the simulated  
520 water storage and all simulated inflows to the catchment. We monitored the water mass conservation  
521 level in the same real catchment as was adopted for model determinism assessment (section 2.3.2,  
522 Model determinism) at the daily time step, considering that the difference between the above two  
523 volumes should remain below 0.001% of the total inflow volume.

## 524 **2.4 Model evaluation**

525 Model evaluation determines the ability to simulate hydrological and agricultural functioning in a real  
526 case study. Basically, the evaluation relies on the comparison of simulated variables to available  
527 observed, or reference, data. As the primary intention in using MHYDAS-Small-Reservoirs is to  
528 quantify the cumulative effects of reservoirs on crop yields and on stream runoff at the catchment

529 outlet, we chose these two variables to evaluate the model. The evaluation therefore followed two  
 530 steps. The first step involved the evaluation of the model in the simulation of global variables  
 531 corresponding to the annual fluxes across the entire catchment for which reference data were available  
 532 for the case study. In the second step, the model ability to finely simulate the daily stream runoff was  
 533 analysed using the Nash-

534 follows: Sutcliffe efficiency (1970) calculated as  
 535

$$NSE_q = 1 - \frac{\sum_{i=1}^n (q_i^s - q_i^o)^2}{\sum_{i=1}^n (q_i^s - \bar{q}^o)^2}$$

536

537 where  $NSE_q$  is the Nash-Sutcliffe efficiency of the stream runoff,  $q_i^o$  is the reference stream runoff at  
 538 the  $i^{\text{th}}$  time index,  $q^o$  is the mean reference stream runoff and  $q_i^s$  is the simulated stream runoff at the  
 539  $i^{\text{th}}$  time index. The closer the value is to 1, the higher the quality of the stream runoff simulation is. The  
 540 efficiency considering the square root of the stream runoff, denoted as  $NSE_{sqrt}$ , was also calculated  
 541 since it assigns a high weight to low values of the stream runoff when  $NSE_q$  is highly sensitive to high  
 542 flows (Oudin et al., 2006; Pushpalatha et al., 2012).

543 When applying the model to the Gélon catchment, the efficiencies were calculated based on the daily  
 544 stream runoff over the full hydrologic year of 2014/2015 starting on 1 September. The daily simulated  
 545 stream runoff,  $q_i^s$ , was calculated as the sum of hourly simulated stream runoff for the  $i^{\text{th}}$  day. As we  
 546 determined that the stream runoff data used as reference data were less reliable between June and  
 547 October and for stream runoff below the threshold of 0.086 mm/d (cf section [2.1.2](#)), we also calculated  
 548 the efficiencies by considering those days when the stream runoff exceeded the above threshold,  
 549 excluding the period from June to October.

## 550 **2.5 Numerical explorations**

551 The model was then applied to simulate, in the Gélon catchment, two situations that differed in terms  
 552 of crop allocation and reservoir water management (Table 3). The objective was to analyse the  
 553 capacity of the model to predict possible future conditions and assess the potential consequences of

554 different policies in crop and agricultural water management strategies, as is commonly achieved in  
 555 scenario exercises using models in water resource management (Leenhardt et al., 2012). The  
 556 “Reference” situation represents the current state, as simulated for the 2014-15 hydrological year,  
 557 which is compared to the second situation, named “All-RE”. The All-RE situation was not designed to  
 558 be realistic but for its illustrative potential. In this situation, we therefore assumed that all reservoirs of  
 559 the catchment were used for irrigation purposes and that all agricultural SUs within a radius of 500 m  
 560 around every RE were irrigated and cropped with maize, the most irrigated crop in the region. The All-  
 561 RE situation thus differs from the Reference situation both in terms of number of reservoirs considered  
 562 for irrigation and in terms of crops and cropping area.

563 **Table 3:** Reservoir and crop and irrigated area characteristics of the “Reference” and “All-RE”  
 564 situations simulated with MHYDAS-Small-Reservoirs in the Gélon catchment

565

Situations	Reference	All-RE
Reservoirs	25 reservoirs, including 13 used for irrigation (164,300 m <sup>3</sup> )	25 reservoirs (206,800 m <sup>3</sup> ) for irrigation purposes
Crop distribution	straw cereals (617 ha) sunflower (497 ha) maize (25 ha) soja (108 ha) other crops (142 ha) set aside (52 ha)	maize (1,067 ha) other crops (405 ha) set aside (21 ha)
Irrigated area	288 ha including: <ul style="list-style-type: none"> <li>● straw cereals (213 ha)</li> <li>● soybeans (16 ha)</li> </ul>	1,056 ha including: <ul style="list-style-type: none"> <li>● maize only</li> </ul>

	<ul style="list-style-type: none"> <li>• maize (14 ha)</li> <li>• rapeseed (7 ha)</li> <li>• sorghum (3 ha)</li> <li>• other crops (35 ha)</li> </ul>	
--	---	--

566

## 567 **3. Results**

### 568 **3.1 Model verification**

#### 569 **3.1.1 Simulator testing, model determinism and water volume conservation**

570 Testing of all the simulators was successful since the variables simulated with the model matched the  
571 expected values. The results are not presented but are available upon request. The model determinism  
572 was verified since the simulated variables in terms of the total water storage in the GUs, SUs and REs  
573 and water fluxes (surface runoff in the SUs and stream runoff in the RSs) were strictly identical for all  
574 1,000 simulations. Water volume conservation in the simulations was also verified: at the annual scale,  
575 the error was lower than 0.0001 % of the inflow volume.

#### 576 **3.1.2 Computation time**

577 The simulation was performed based on an Ubuntu Quad-Core microprocessor at 2.90 GHz, with  
578 128 GB of RAM and a 32-bit CPU. The computation time reached 17 hours for a 26-year period in the  
579 Gélon catchment, with a display of the daily global variables in the whole domain and an additional  
580 display of all of the variables in each spatial unit (3 per RS and GU, 7 per RE and 30 per SU) for the  
581 last simulated year, which represents 4.7 Go.

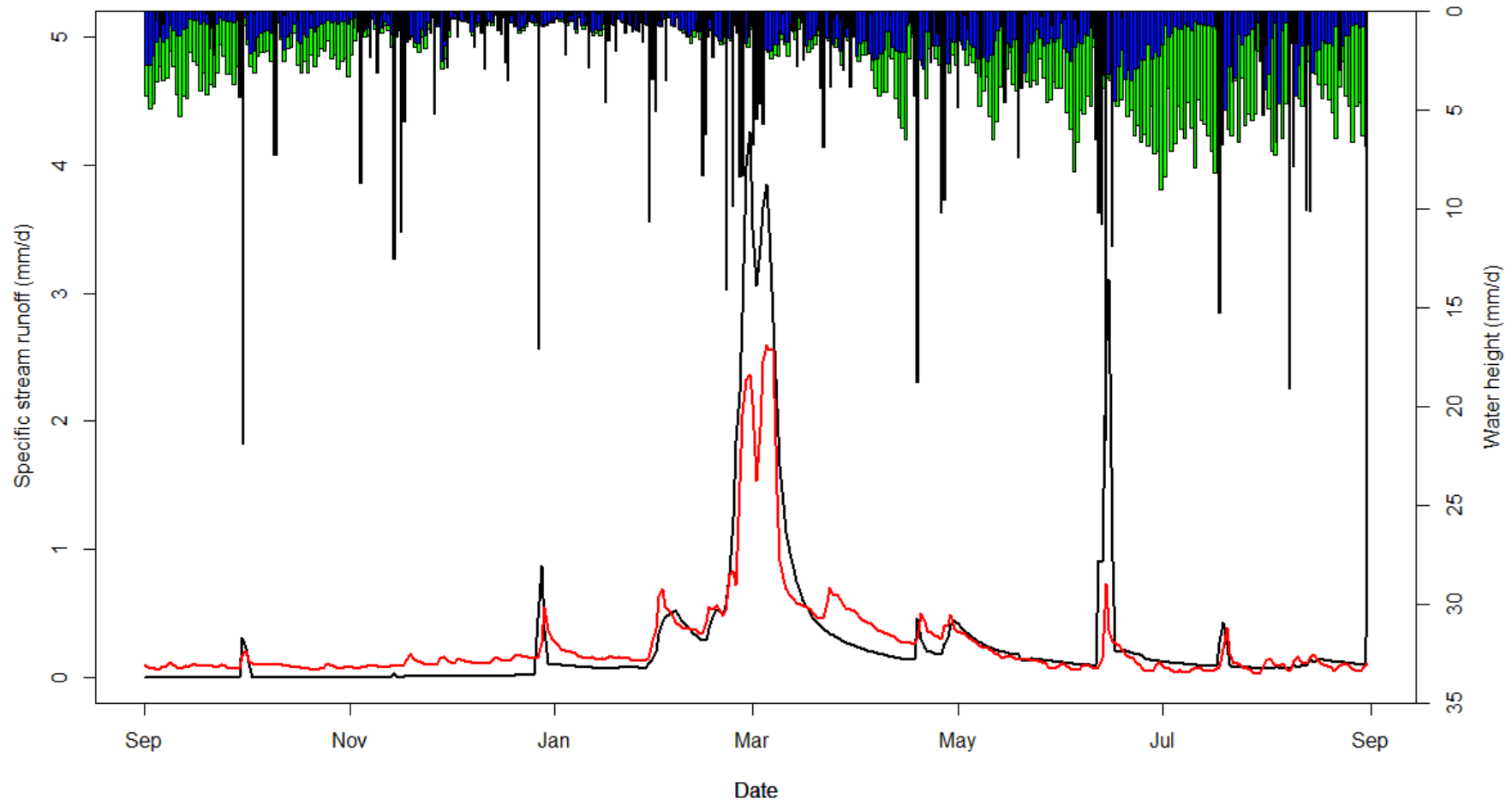
### 582 **3.2 Model evaluation**

583 At the catchment level, the simulated stream runoff over the hydrological year of 2014/2015 is 102.8  
584 mm (Table 4), which is only 6.4% higher than the reference stream runoff (96.6 mm). The efficiencies  
585 of  $NSE_q$  and  $NSE_{sqrq}$  of the simulated daily stream runoff are 0.32 and 0.26, respectively. In regard to

586 the days when the stream runoff exceeds 0.086 mm/d between November and May, when the  
 587 reference stream data are considered reliable (please refer to section 2.4), the calculated  $NSE_q$  and  
 588  $NSE_{sqrq}$  values are both 0.47. These values approaching 0.5 indicate that the model yields nearly  
 589 satisfactory results not only for high flows, in terms of  $NSE_q$  (Moriassi et al., 2015), but also for low  
 590 flows, in terms of  $NSE_{sqrq}$  (Oudin et al., 2006). Over the period corresponding to these days, the  
 591 simulated daily stream runoff matches the reference stream runoff well (Figure 5). During this period,  
 592 the simulated cumulative stream runoff is 82.6 mm, which is 3.3% higher than the cumulative  
 593 reference stream runoff (80.0 mm). According to Moriassi et al. (2015), an error of less than 5% is  
 594 considered very good. On the basis of all the efficiencies and differences between the simulation and  
 595 reference data, the model applied to the Gélon catchment yields acceptable or even good simulations  
 596 of the hydrology.

597 **Table 4:** Catchment water balance terms simulated for the two situations of the Gélon catchment for  
 598 the hydrologic year 2014/2015. The simulated AET, stream runoff at the outlet, irrigation and storage  
 599 variation between the start and the end of the simulation period are expressed in mm. The rainfall and  
 600  $ET_0$ , as input variables, are also indicated and expressed in mm. For irrigation, the value in brackets  
 601 indicates the mean annual irrigation per irrigated plot area (mm).

Situations	AET ( $ET_0$ )	Rainfall	Stream runoff	Storage variation	Irrigation
<b>Reference</b>	436.4 (960.7)	570.7	102.8	+31.5	4.2 ( <b>28.9</b> )
<b>All-RE</b>	473.9 (960.7)	570.7	97.0	-0.1	7.1 ( <b>13.3</b> )



602  
603

604

605 **Figure 5:** Simulated (black line) and reference (red line) daily specific stream runoff (mm/d) at the Gélon catchment outlet for the hydrologic year of  
606 2014/2015. The daily rainfall (in black), ET0 (in green) and AET (in blue) are also represented (in mm/d) on the right inverted y-axis.

607 Table 5 summarizes the simulated and regionally observed crop yields. Considering all the crops, the  
 608 area-weighted average of the relative root mean square errors across the Gélon catchment is 21.4%,  
 609 which is quasi-acceptable according to Cabelguenne et al. (1990) and Constantin et al. (2015), who  
 610 considered a difference of 20% between the observed and simulated yields acceptable. This  
 611 performance results from the good performance of the model in the simulation of the sunflower and  
 612 sorghum yields and the poor yield simulation performance for soybeans, rapeseed, maize and straw  
 613 cereals.

614 **Table 5:** Simulated and regionally observed crop yields in the Gélon catchment, accounting for 86.1%  
 615 of the crop area. The regionally observed crop yields correspond to data retrieved from the Gers  
 616 department in 2015 (DRAAF Occitanie, 2020), considering the maize yield in proportion to the  
 617 irrigated and non-irrigated maize areas in the Gélon catchment.

Species	Regionally observed yield (T.ha <sup>-1</sup> )	Simulated yield (T.ha <sup>-1</sup> )	Yield error (%)	Cultivated area (%)
Soybeans	3.50	2.21	-37%	7.28%
Sunflower	1.70	1.45	-15%	33.28%
Rapeseed	2.5	3.30	+32%	0.45%
Sorghum	5.5	5.84	+6%	2.12%
Maize	8.4	5.43	+35%	1.65%
Straw cereals	5.4	6.70	+24%	41.30%

### 618 3.3 Numerical experiment results

#### 619 3.3.1 Global variables

620 The annual catchment water balance terms in the two situations are reported in Table 4. The simulated  
 621 irrigation amounts rank as expected with the largest volume occurring in the All-RE situation, due to  
 622 both the large irrigated area and abundant available water resources. The simulated stream runoff in  
 623 the All-RE situation was 6% lower than in the Reference situation.



624 The crop yield varies both between crops within a situation and between the two situations (Table 6).  
 625 In the All-RE situations, yields of non-irrigated crops (i.e., sunflower) are not very different from  
 626 those in the Reference situation (<2%) since a rainfed crop in the reference situation remains non-  
 627 irrigated in All-RE. Crops irrigated on only part of their area in the Reference situation are either  
 628 replaced by irrigated maize or maintained as non-irrigated in the All-RE situation. As a result, when  
 629 they do not disappear (as for rapeseed and sorghum), their yield decreases slightly if they were lightly  
 630 irrigated (e.g., straw cereals) or considerably if they were intensively irrigated (e.g., soybeans).  
 631 Regarding maize, the yield decrease observed in All-RE (-12% compared to the Reference) has  
 632 another explanation. In All-RE, the number of reservoirs for irrigation increased, and all irrigated  
 633 surfaces were converted into maize crop plots. The increase in the overall volume of water available  
 634 for irrigation purposes did not compensate for the increase in the total water demand resulting from the  
 635 increase in the area of irrigated maize, hence the decrease in yield.

636 **Table 6:** Variations in the crop yields in the Gélon catchment considering the two simulated  
 637 situations. The values are given in T/ha but also in T at the catchment scale. Variations are also given  
 638 in percent compared to the Reference situation.

	Soybeans	Sunflower	Rapeseed	Sorghum	Maize	Straw cereals
Reference	2.21 T/ha <b>240 T</b>	1.45 T/ha <b>720 T</b>	3.30 T/ha <b>22 T</b>	5.84 T/ha <b>185 T</b>	5.43 T/ha <b>134 T</b>	6.70 T/ha <b>4,131 T</b>
All-RE	1.99 T/ha (-10.0%) <b>119 T</b>	1.47 T/ha (+1.4%) <b>213 T</b>	-	-	4.78 T/ha (-12.0%) <b>5,100 T</b>	6.70 T/ha (0.0%) <b>1,048 T</b>

### 639 3.3.2 Spatially distributed variables

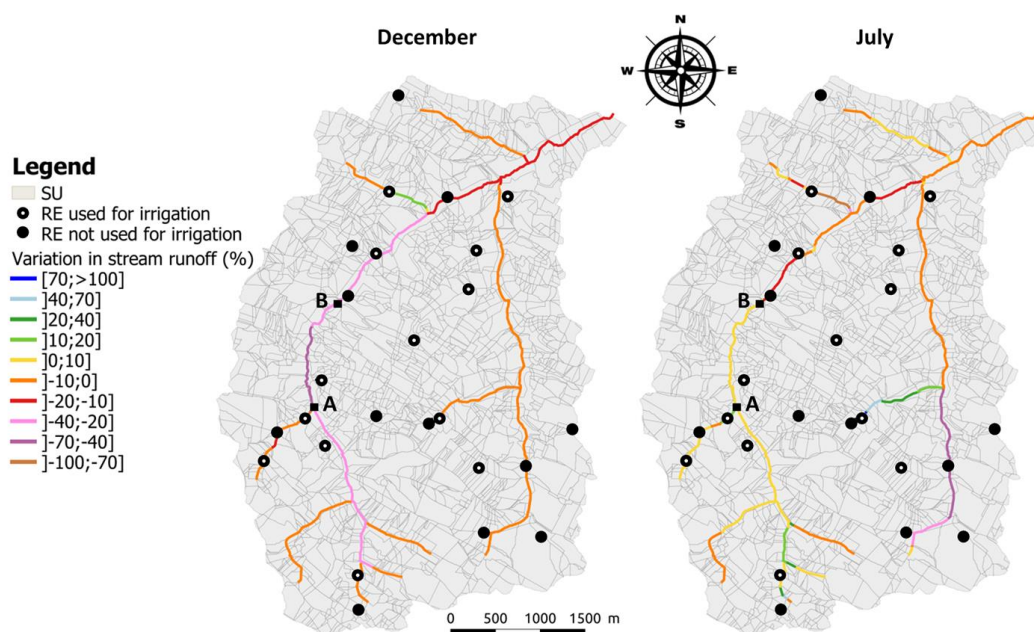
640 MHYDAS-Small-Reservoirs simulates a large number of spatially distributed variables related to the  
 641 hydrological and agricultural responses of a catchment. We illustrate three of them, namely, i) stream  
 642 runoff, ii) irrigation water demand and iii) reservoir filling rate evolution.

643 The stream runoff is simulated along the whole hydrographic network at the RS resolution. This  
644 allows us to assess and compare the inner-catchment variability, as shown in Figure 7, where the  
645 difference in the monthly stream runoff along the hydrographic network between the Reference and  
646 All-RE situations in December 2014 and July 2015 is plotted. These two months were chosen because  
647 they corresponded to high flow and low flow periods, respectively. In that respect, several results can  
648 be highlighted. The first result is that the relative variation in the monthly stream runoff between the  
649 situations at the catchment outlet differs from one month to another and that the variation in the annual  
650 stream runoff also differs. For example, although the simulated annual runoff in the All-RE situation  
651 was lower by -6% compared to the Reference situation, the difference of monthly stream runoff  
652 between both situations was -3% in July and -14% in December. The second notable result is that the  
653 variation in the stream runoff at the outlet may mask the high variability in stream runoff along the  
654 hydrographic network. The simulated stream runoff variation was negative in most of the stream  
655 reaches (Figure 7), indicating a lower stream runoff in the All-RE situation than in the Reference  
656 situation over the two months analysed. This result was expected due to i) the higher crop water  
657 requirement of maize compared to the straw cereals, which is the main irrigated crop in the Reference  
658 situation, and ii) the larger water withdrawals in the reservoirs in order to irrigate maize. This leads to  
659 emptier reservoirs at the beginning of the rainy period and thus to an increase of water interception of  
660 runoff and stream runoff by the reservoirs and to a decrease of the stream runoff in the catchment.  
661 However, in July, in the western branch of the hydrographic network, delimited by A and B in Figure  
662 7, the stream runoff was higher (+9%) than that in the Reference situation. This counterintuitive result  
663 is explained by an increase of the baseflow in the All-RE situation, which is 8% higher in July for  
664 certain GUs in the southwest of the catchment. This increase in the baseflow is first related to the  
665 irrigation. Indeed, the absence of irrigation under the Reference situation in the northwest of the  
666 catchment (Figure 7) leads to a lower soil water content than that in the All-RE situation, where the  
667 soils are cropped with highly irrigated maize. The rainfall in July and the subsequent infiltration  
668 allows the soil water content to exceed the soil field capacity faster, thus triggering larger soil  
669 percolation in the All-RE situation than in the Reference. However, this phenomenon is limited to a

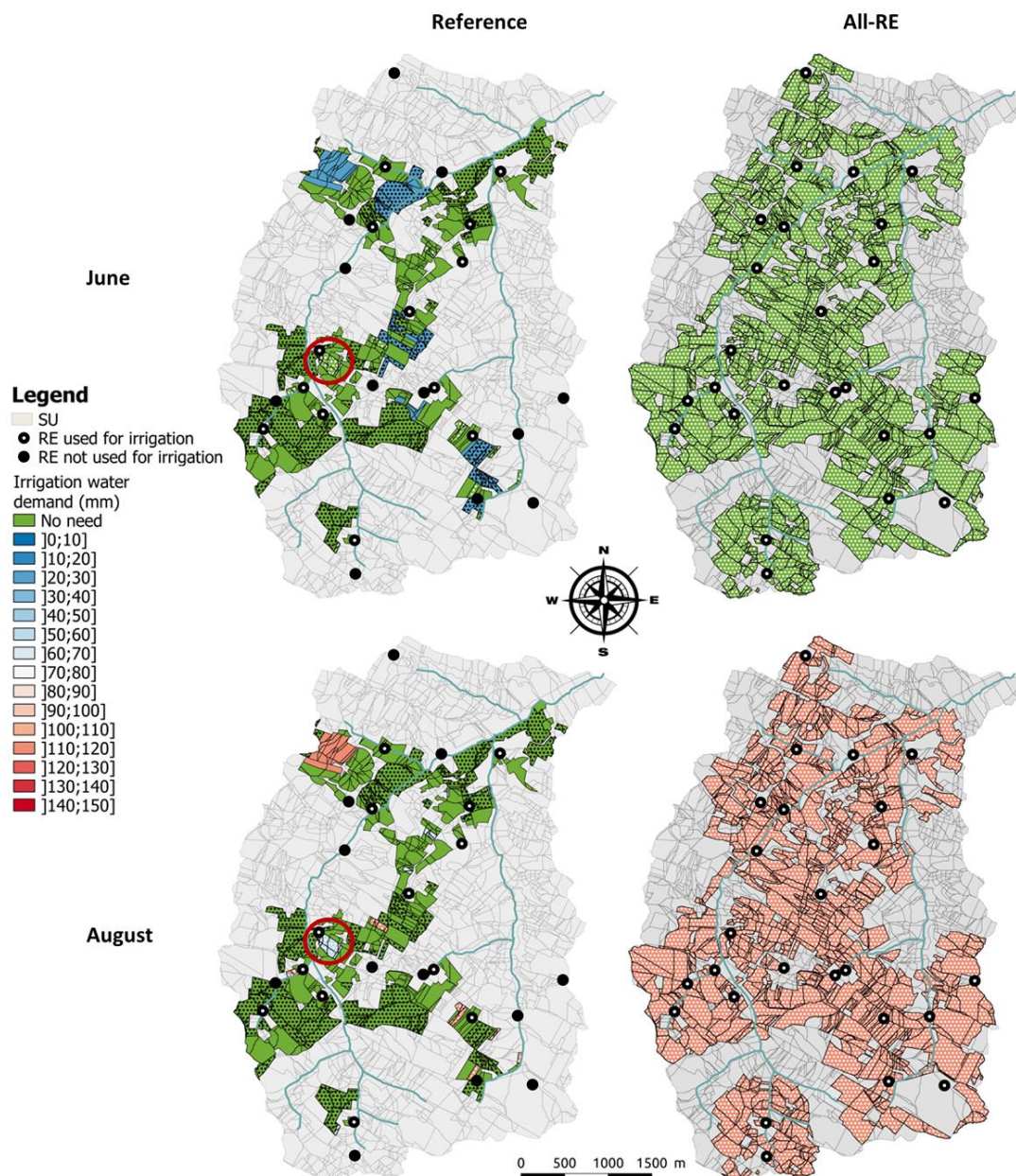
670 small part of the catchment. Indeed, in the rest of the catchment, the water amount available for  
671 irrigation in the reservoirs is smaller than the demand, and the mean soil water content in the All-RE  
672 situation remains lower than that in the Reference situation. Thus, at the catchment scale, the stream  
673 runoff is slightly modified by these changes and driven more by the increasing AET due to the maize  
674 crops.

675 The irrigation water demand also exhibits inner spatial and temporal variability, as shown in Figure 7,  
676 where the irrigation water demand is plotted for the Reference and All-RE situations and two months  
677 corresponding to the beginning (June) and the end (August) of the irrigation period. These two months  
678 illustrate well how the water demand depends on crop requirements and water resource availability in  
679 reservoirs, which usually decreases with time during the irrigation period . The water demand is quite  
680 uniform in the catchment for the All-RE situation because all irrigated fields are cropped with the  
681 same crop, maize. The difference in water demand between June and August relies mainly on this  
682 situation in crop water requirements. In June, the maize was planted a few weeks earlier, and the crop  
683 water requirement, and thus the water demand for irrigation, is low. In August, the crop requirement is  
684 large due to the crop development and the high  $ET_0$  (Figure 5). As the reservoirs are empty at this  
685 time (Figure 8), the water demand remains high most of the time. In the reference situation, water  
686 demand is slightly more variable than for the All-RE situation because there are different irrigated  
687 crops, such as straw cereals, soybean and maize. The crop development in time and the irrigation  
688 period are different from one crop to another one. As straw cereals are harvested in July, all fields with  
689 this crop are simulated with a zero water demand in August for the reference situation (fields with  
690 black dots in the left map of Figure 7). As in the All-RE situation, the temporal variation in water  
691 demand for maize fields between June and August also results from the water availability in the  
692 reservoirs. For instance, the simulated water demand for the field in maize indicated by a red circle in  
693 Figure 7 varies from zero in June to more than 60 mm in August. The water volume in the reservoir  
694 connected to this field (grey line in Figure 8) is not large enough in August to meet the crop  
695 requirement, leading to a permanent high water demand.

696 The reservoir filling rate, which is the ratio between the volume of water stored and the RE capacity,  
697 also reveals a high spatial and temporal variability (Figure 8). This finding is explained by the spatial  
698 distribution of the crops, the different water requirements and cycles of the different crops, and the  
699 locations and properties of the reservoirs. Whether a reservoir is used for irrigation or not is the first  
700 variation factor of the filling rate between reservoirs: either connected or non-connected, REs remain  
701 almost full throughout the year as long as they are not applied for irrigation purposes (the blue and red  
702 curves in Figure 8b). The type of irrigated crop is the second factor, namely, in the Reference  
703 situation, where the various crops are irrigated, the reservoir levels decrease first in June to irrigate the  
704 straw cereal, market gardening and soybean crops and again from July to September when the maize  
705 and soybean crops are irrigated (the orange, green, grey and black lines in Figure 8b), while in the All-  
706 RE situation with all irrigated plots cropped with maize, the decrease in June is not observed (all the  
707 coloured lines in Figure 8c). The type of reservoir, connected or non-connected, is another factor  
708 explaining the differences in filling rate. When the irrigation water demand is high, as that during  
709 maize irrigation in the All-RE situation, the connected reservoirs (the red and orange lines in Figure 8b  
710 and 8c) are more likely to become filled because they benefit from both surface and stream runoff  
711 from the upstream reach, while the non-connected reservoirs, only receiving surface runoff, are less  
712 likely to become filled (the blue and green lines in Figure 8b and 8c). The last factor is the location of  
713 the reservoir, as illustrated by the difference between two non-connected reservoirs reserved for  
714 irrigation (the black and grey lines, respectively, in Figure 8). In one case (the black line), the drained  
715 area is not large enough to fill the reservoir during the surface runoff period, and the reservoir remains  
716 almost empty throughout the year regardless of the situation. In the second case (the grey line), the  
717 drained area is large enough to support a high filling rate, as indicated by the filling rate approaching  
718 the reservoir capacity during the rainfall events in late June.



719 **Figure 6:** Stream runoff differences simulated along the hydrographic network in two months  
 720 (December 2014 and July 2015) for the All-RE situation. The differences are calculated between the  
 721 mean monthly simulated stream runoffs in each of the situations and the Reference situation. The  
 722 depicted water reservoir units (REs) dedicated to irrigation or not are those in the Reference situation.  
 723 Black squares A and B delimit the western branch of the hydrographic network.

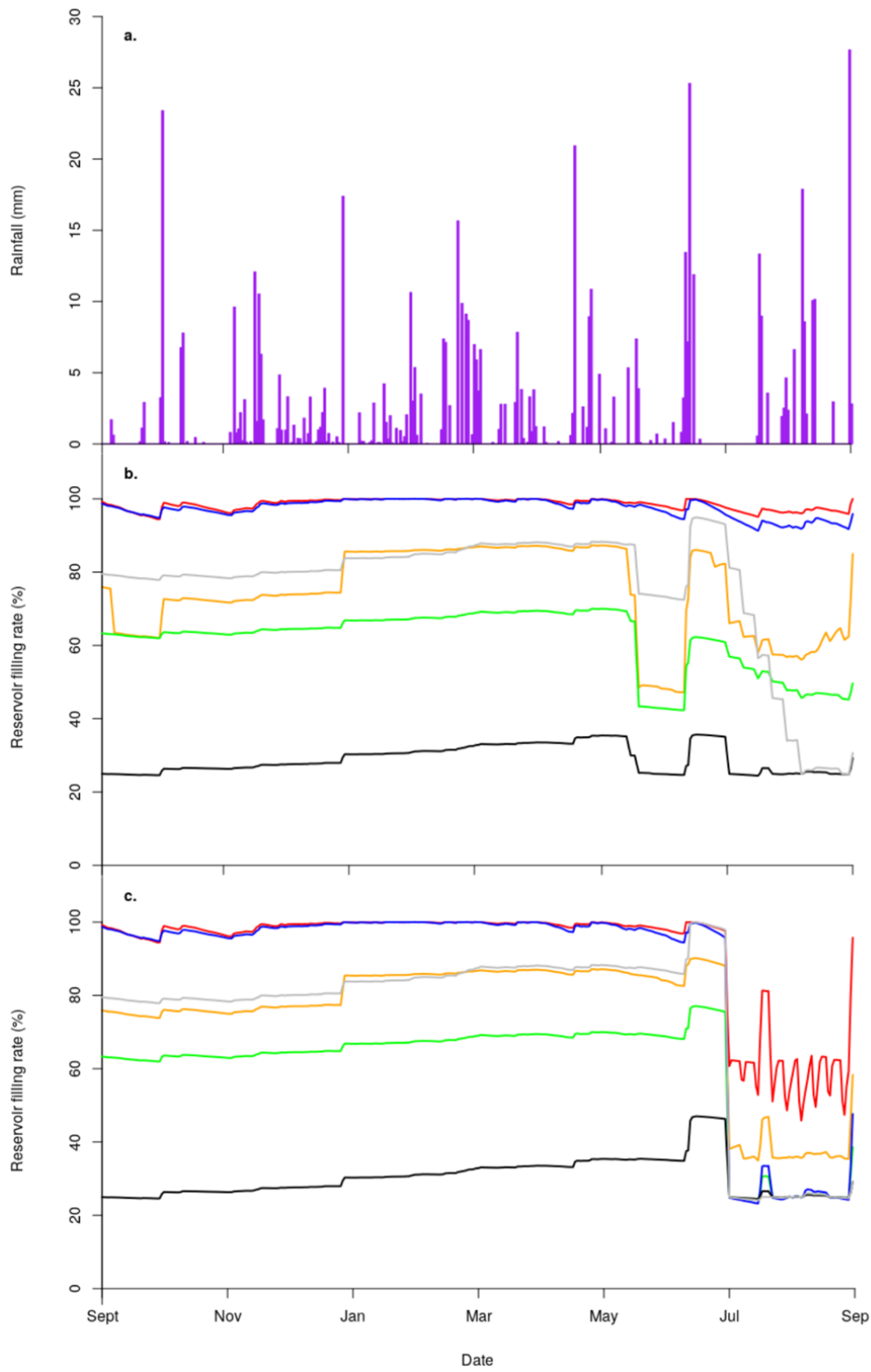


724

725

726 **Figure 7:** Monthly cumulative irrigation water demand simulated in June 2015 and August 2015 in  
 727 the Reference and All-RE situations. The non-irrigated SUs are indicated in grey. The irrigable  
 728 agricultural SUs without a water demand are marked in green. The various colours from dark blue to

729 red indicate a low to high irrigation water demand. The blue lines are the RSs, the black crosses and  
730 the black points are the Res, with a white dot for those dedicated to irrigation. The maize crops are  
731 indicated with white dots and cereals by black dots.



732

733 **Figure 8:** Daily rainfall (a) and variations in water storage in the reservoirs relative to their volume  
734 capacities in the Reference (b) and All-RE (c) situations. The coloured lines indicate the different RE  
735 configurations and groupings defined in the Reference situation, which were maintained in the All-RE  
736 situation. The mean reservoir filling rates are represented for the connected REs reserved for irrigation  
737 (6 REs, orange line), the connected REs not dedicated to irrigation (4 REs, red line), the non-  
738 connected REs dedicated to irrigation (7 REs, green line) and the non-connected REs not dedicated to  
739 irrigation (8 REs, blue line). In addition, the specific reservoir filling rate for two non-connected REs  
740 dedicated to irrigation (in black and grey, respectively) is also plotted.

#### 741 **4. Discussion**

742 The first application of the MHYDAS-Small-Reservoirs model to the Gelon catchment gave  
743 promising results (Figure 5; Tables 4 and 5). The main processes underlying the hydrological and  
744 agricultural functioning of the catchment seem to be well modelled. However, considering the  
745 application of the model to other catchments and other agropedoclimatic contexts requires questioning  
746 (i) the availability of the data needed for its application to other real case studies and (ii) the  
747 improvements to the model in terms of the processes represented. The two points are discussed  
748 hereafter.

749 The first point of discussion concerns the data needed to use the MHYDAS-Small-Reservoirs model,  
750 either to define forcing variables to obtain the spatial representation of the flow domain to  
751 parameterise it on the study area or to evaluate it. Most of the necessary data (e.g., topography,  
752 hydrographic network, soil characteristics, nature of crops, and meteorological variables) may be  
753 extracted or derived from generic databases, often available throughout Europe. Moreover, as this  
754 model is built on already proven models and on widely used equations, some parameters can be fixed  
755 from the literature. For example, this is the case for the plant growing coefficients or for the k factor  
756 for converting reference evapotranspiration to reservoir evaporation. This makes it easy to envision the  
757 use of the model in catchment areas other than the one we studied.



758 However, there is no generic database for all model inputs or for all variables used for its evaluation.  
759 In such cases and when available, those data may be derived from local databases, specific surveys or  
760 local expertise. This is particularly the case for data on reservoirs: there is currently no database at the  
761 European or even the French level that allows a complete and high-quality description of small water  
762 reservoirs. The availability and estimation of the small reservoirs properties and the water use from the  
763 reservoirs have remained a real challenge regardless of the approaches used in catchment hydrological  
764 modelling with reservoirs (Hughes and Mantel, 2010, Lowe et al. 2005). This has motivated the  
765 development of remote sensing methods to estimate position and capacity of small reservoirs over  
766 large areas (Ogilvie et al., 2016). In France, the collective water management structures recently set up  
767 in deficit areas ("Organismes Uniques de Gestion Collective de l'Eau") are beginning to create a type  
768 of database gathering characteristics and water uses of small reservoirs. Databases describing  
769 agricultural practices are also incomplete, either in terms of geographical location or in terms of  
770 content, as explained in Leenhardt et al. (2010, 2020). Therefore, this requires the implementation of  
771 specific acquisition methods, for example, as presented for cropping systems by Murgue et al. (2016)  
772 and Rizzo et al. (2019). It is clear that the lack of generic databases for some of the necessary variables  
773 to use or evaluate the model makes using the model more difficult. However, this constraint is not  
774 specific to MHYDAS-Small-Reservoirs and has been encountered by other modelling approaches  
775 dealing with the cumulative effect of small reservoirs.

776 The quality of the data used also guarantees the predictive quality of the model and the reliability of  
777 the model assessment. The use of indirect acquisition methods necessarily introduces inaccuracies,  
778 either because of the quality of the expertise (Rizzo et al., 2019) or because of the method itself. For  
779 example, in our case study, we did not manage to meet all the owners of the reservoirs (absences or  
780 refusals) so that the data for some reservoirs correspond to hypotheses based on our observations or on  
781 the expertise of neighbours. However, the existence of generic databases does not exclude the need to  
782 examine the quality of the data included in them. For example, in the present study, although we had  
783 databases providing stream flow, meteorological data and crop yield values, we were only able to

784 access stream flow data at a nearby station located within the same basin but outside the Gélon  
785 catchment, while meteorological data and crop yield values, respectively, were at a resolution that was  
786 too low to obtain internal spatial variability on an 8 km<sup>2</sup> grid and averaged over the entire Gers  
787 department,. These spatial discrepancies necessarily affect the quality of the data. More intensive field  
788 work, for example, by monitoring flows at the Gélon outlet or by obtaining yield values from  
789 agricultural cooperatives or traders who collect crops in this sector, would have enabled a better  
790 evaluation of the model's performance.

791 The second point of discussion is about the way to improve the modelling of processes in MHYDAS-  
792 Small-Reservoirs, in particular processes directly affecting the reservoir. Regarding this point, the  
793 modular design of the MHYDAS-Small-Reservoirs model under the OpenFLUID platform easily  
794 allows adding or improving simulators. In the current version of the model, some processes are  
795 neglected. This is the case for infiltration of water from the reservoirs to the underlying groundwater  
796 or conversely for the discharge of groundwater directly to the reservoirs. Neglecting these processes  
797 appeared to be acceptable in the Gélon catchment given the characteristics of the reservoirs and their  
798 connection to the groundwater. However, depending on the pedological and lithological contexts and  
799 the properties of the reservoirs, in particular the hydrodynamic properties of the reservoir bed,  
800 exchanges between the reservoir and the groundwater can be dominant processes in the hydrological  
801 dynamics of the reservoir (Bouteffeha et al., 2015). Modelling the exchanges would therefore improve  
802 the model in its ability to simulate a diversity of contexts. The modelling could be done simply by  
803 considering the differences in water levels between the reservoir and groundwater. This type of  
804 relationship is reported to well predict the dynamics of exchanges in various contexts (Sharda et al.,  
805 2006).

806 Another improvement of the model is in the modelling of the water management rules of the  
807 reservoirs. Indeed, the cumulative hydrological effect of reservoir networks cannot be explained solely  
808 by the geometric characteristics of the network (density in terms of number of reservoirs, volume or  
809 surface area). The management rules of the reservoirs, which sometimes differ from one reservoir to

810 another, appear to be an important factor in this effect (Habets et al., 2018; Hughes and Mantel, 2010).  
811 In the present case study, the sharing of available water in a reservoir is modelled by a fairly standard  
812 approach by considering that the water withdrawn is distributed to the irrigated field proportionally to  
813 the water demand, but other priority rules could be considered. Priority could be given, for example, to  
814 crops providing high financial incomes. We could also consider defining rules based on short-term  
815 weather predictions. For actual water management rules being modelled within a specific simulator,  
816 the modular design of the MHYDAS-Small-Reservoirs model will be a clear asset to allow various  
817 water management modalities.

## 818 **5. Conclusions**

819

820 The MHYDAS-Small-Reservoirs model has been developed to understand and predict the local and  
821 cumulative hydrologic and agricultural effects of a reservoir network in an agricultural catchment.  
822 Hydrological models are already available to assess the cumulative impact of reservoir networks.  
823 Compared to these models, the originality of MHYDAS-Small-Reservoirs lies in two of its features.  
824 The first is that it integrates processes related to the three major components of the catchment's agro-  
825 hydrological functioning: hydrology, crop growth, and water management decisions. The second  
826 feature is that it explicitly represents the main elements of the agricultural catchment - the plot, the  
827 reach, the reservoir, and the water table - and the hydrological and agricultural relationships between  
828 these elements. In addition, the model distinguishes between reservoirs according to their connection  
829 to the hydrographic networks. In doing so, it allows the simulation of both local effects in the  
830 immediate environment of each reservoir and cumulative effects on overall yields (Table 6) and flows  
831 (Figure 6).

832 Numerical verification of the model was successful. The first application of the model to a 19-km<sup>2</sup>  
833 catchment gave promising results in terms of stream runoff and crop yield simulations. However, the  
834 evaluation and validation of the model are incomplete. The model could be improved in two

835 directions. The first concerns its validation, with an analysis of the model performance to simulate the  
836 variables for which it was intended, such as stream runoff, crop yields and water withdrawals and  
837 availability in small reservoirs. Model validation could also gain from its application to catchments  
838 where comprehensive, reliable and distributed data sets, such as water tables, stream runoff and crop  
839 yield data, are available based on in situ measurements and observations. The second direction would  
840 be to perform a sensitivity analysis. In particular, a sensitivity analysis of the reservoir characteristics  
841 and of the parameters associated with water dynamics modelling in small reservoirs could be helpful  
842 when parameterizing the model in future applications. Thus, the MHYDAS-Small-Reservoirs model  
843 could potentially be adopted by land use planners and water managers to assist them in their decisions  
844 regarding new small-reservoir projects in catchments or management of the water stored in reservoirs.

845

#### 846 **Acknowledgements:**

847 This work was financed by a PhD scholarship from the French Occitanie-Pyrénées-Méditerranée  
848 Region and the French National Research Institute for Agriculture, Food and Environment (INRAE).  
849 A part of this work was financed by the French Biodiversity Agency (Office Français pour la  
850 Biodiversité). The authors thank the Compagnie d'Aménagement des Coteaux de Gascogne (CACG)  
851 and MeteoFrance for access to their databases.

852 We would like to thank Jean-Christophe Fabre, OpenFLUID team leader, for his help and contribution  
853 to the development of the MHYDAS-Small-Reservoirs. Also, special thanks to Romain Lardy, Marie  
854 Estienne, Manuel Chataigner and Ekaterina Ferry-Zadonina for their help in the modelling work and  
855 to Koladé Akapko, Victor Giffone and LISAH technicians Sébastien Troiano, David Fages and Olivier  
856 Huttel for facilitating the in situ data collection.

#### 857 **Software and data availability**

858 MHYDAS-Small-Reservoirs runs with the OpenFLUID platform. OpenFLUID is a software  
859 environment for modelling and simulation of complex landscape systems. The documentation and

860 versions of OpenFLUID platform can be found on the OpenFLUID site at [www.openfluid-project.org](http://www.openfluid-project.org).  
861 A dedicated GitHub workspace is also available at <https://github.com/OpenFLUID/openfluid>. The  
862 GitHub workspace dedicated to MHYDAS-Small-Reservoir is available at <https://github.com/UMR->  
863 LISAH/MHYDAS-Small-Reservoirs.

864 **References**

- 865 Agence de l'Eau, French Ministry of the Environment, SANDRE, and IGN. 2014. 'BD CarTHAgE'.  
 866 Base de Données sur la CARTographie THématique des AGences de l'Eau et du ministère chargé  
 867 de l'environnement.  
 868 <http://services.sandre.eaufrance.fr/telechargement/geo/ETH/BDCarthage/FXX/2014/>.
- 869 Ajami, Hoori, Matthew F. McCabe, Jason P. Evans, and Simon Stisen. 2014. 'Assessing the Impact of  
 870 Model Spin-up on Surface Water-Groundwater Interactions Using an Integrated Hydrologic  
 871 Model'. *Water Resources Research* 50 (3): 2636–56. <https://doi.org/10.1002/2013WR014258>.
- 872 Algayer, Baptiste, Philippe Lagacherie, and Jean Lemaire. 2020. 'Adapting the Available Water  
 873 Capacity Indicator to Forest Soils: An Example from the Haut-Languedoc (France)'. *Geoderma*  
 874 357 (January): 113962. <https://doi.org/10.1016/j.geoderma.2019.113962>.
- 875 Allain, S., Obiang Ndong, G., Lardy, R., Leenhardt D., 2018. Integrated assessment of four strategies  
 876 for solving water imbalance in an agricultural landscape. *Agron. Sustain. Dev.* 38: 60.  
 877 <https://doi.org/10.1007/s13593-018-0529-z>
- 878 Beven, Keith, and Andrew Binley. 1992. 'The Future of Distributed Models: Model Calibration and  
 879 Uncertainty Prediction'. *Hydrological Processes* 6 (3): 279–98.  
 880 <https://doi.org/10.1002/hyp.3360060305>.
- 881 Biemans, Hester, Ingjerd Haddeland, Pavel Kabat, Fulco Ludwig, Ronald W. A. Hutjes, Jens Heinke,  
 882 Werner von Bloh, and Dieter Gerten. 2011. 'Impact of Reservoirs on River Discharge and  
 883 Irrigation Water Supply during the 20th Century'. *Water Resources Research* 47 (3).  
 884 <https://doi.org/10.1029/2009WR008929>.
- 885 Bouvet, Lionel, Xavier Louchart, Martin Barès, Sylvain Lalauze, Roger Moussa, and Marc Voltz.  
 886 2010. 'Modélisation intégrée des agro-hydrosystèmes avec MHYDAS: Exemple Des Transferts

- 887 de Pesticides En Milieu Viticole Méditerranéen’. In *Proceedings of the 40th Colloquium of the*  
 888 *GFP*. Banyuls-sur-Mer, France: Cooper, J.F. et al, 2010.
- 889 Brighenti, Tássia Mattos, Nadia Bernardi Bonumá, Raghavan Srinivasan, and Pedro Luiz Borges  
 890 Chaffe. 2019. ‘Simulating Sub-Daily Hydrological Process with SWAT: A Review’.  
 891 *Hydrological Sciences Journal* 64 (12): 1415–23.  
 892 <https://doi.org/10.1080/02626667.2019.1642477>.
- 893 Cabelguenne, Maurice, Charles Allan Jones, Jean-Robert Marty, Paul T. Dyke, and Jimmy R.  
 894 Williams. 1990. ‘Calibration and Validation of EPIC for Crop Rotations in Southern France’.  
 895 *Agricultural Systems* 33 (2): 153–71. [https://doi.org/10.1016/0308-521X\(90\)90078-5](https://doi.org/10.1016/0308-521X(90)90078-5).
- 896 Cavailé, Albert, and BRGM. 1968. ‘Note on the geological map of Beaumont-de-Lomagne (Notice de  
 897 la carte géologique de Beaumont-de-Lomagne)’. Detailed geological map of France N°955.  
 898 France: BRGM. <http://ficheinfoterre.brgm.fr/Notices/0955N.pdf>.
- 899 Çetin, Lydia T., Andrew C. Freebairn, Phillip W. Jordan, and Bianca J. Huider. 2009. ‘A Model for  
 900 Assessing the Impacts of Farm Dams on Surface Waters in the WaterCAST Catchment  
 901 Modelling Framework’. In *18th World IMACSMODSIM Congress*, 3478–84. Cairns, Australia.  
 902 <http://mssanz.org.au/modsim09>.
- 903 Chiarelli, Davide Danilo, Corrado Passera, Lorenzo Rosa, Kyle Frankel Davis, Paolo D’Odorico, and  
 904 Maria Cristina Rulli. 2020. ‘The Green and Blue Crop Water Requirement WATNEEDS Model  
 905 and Its Global Gridded Outputs’. *Scientific Data* 7 (1): 273. [https://doi.org/10.1038/s41597-020-](https://doi.org/10.1038/s41597-020-00612-0)  
 906 [00612-0](https://doi.org/10.1038/s41597-020-00612-0).
- 907 Chow, Ven T. 1959. *Open-Channel Hydraulics*. First edition. New York: McGraw-Hill.
- 908 Constantin, Julie, Magali Willaume, Clément Murgue, Bernard Lacroix, and Olivier Therond. 2015.  
 909 ‘The Soil-Crop Models STICS and AqYield Predict Yield and Soil Water Content for Irrigated

- 910 Crops Equally Well with Limited Data'. *Agricultural and Forest Meteorology* 206 (June): 55–68.  
 911 <https://doi.org/10.1016/j.agrformet.2015.02.011>.
- 912 Deitch, Matthew J., Adina M. Merenlender, and Shane Feirer. 2013. 'Cumulative Effects of Small  
 913 Reservoirs on Streamflow in Northern Coastal California Catchments'. *Water Resources  
 914 Management* 27 (November): 5101–18. <https://doi.org/10.1007/s11269-013-0455-4>.
- 915 DRAAF Occitanie. 2020. 'French Annual Agricultural Statistics - Areas, yields and production from  
 916 2000 to 2019 by department of Occitanie for cereals, oilseeds and protein crops (Statistique  
 917 Agricole Annuelle (SAA) - Surfaces, rendements et production de 2000 à 2019 par département  
 918 d'Occitanie des céréales, oléagineux, protéagineux)'. Edited by French Ministry of Agriculture.  
 919 Statistical data of the SRISET Occitanie. [http://draaf.occitanie.agriculture.gouv.fr/Cereales-](http://draaf.occitanie.agriculture.gouv.fr/Cereales-oleagineux)  
 920 [oleagineux](http://draaf.occitanie.agriculture.gouv.fr/Cereales-oleagineux).
- 921 Durand, Yves, Eric Brun, Laurent Merindol, Gilbert Guyomarc'h, Bernard Lesaffre, and Eric Martin.  
 922 1993. 'A Meteorological Estimation of Relevant Parameters for Snow Models'. *Annals of  
 923 Glaciology* 18: 65–71. <https://doi.org/10.1017/S0260305500011277>.
- 924 Fabre, Jean-Christophe, Armel Thöni, and David Crevoisier. 2020. 'OpenFLUID'. Documentation.  
 925 OpenFLUID: Modelling Fluxes in Landscapes. September 2020. [https://www.openfluid-](https://www.openfluid-project.org/)  
 926 [project.org/](https://www.openfluid-project.org/). (accessed 9.9.20).
- 927 Fabre, Jean-Christophe, Xavier Louchart, François Colin, Cécile Dagès, Roger Moussa, Michael  
 928 Rabotin, Damien Raclot, Philippe Lagacherie, and Marc Voltz. 2010. 'OpenFLUID : A Software  
 929 Environment for Modelling Fluxes in Landscapes'. In *International Conference on Integrative  
 930 Landscape Modelling*, 1–13. Montpellier: Quae ; INRA ; CIRAD.  
 931 <http://www.documentation.ird.fr/hor/fdi:010051568>.
- 932 Faivre, Robert, Claude Bruchou, Jean Couteau, Nicolas Dumoulin, Thierry Faure, Bertrand Ioss,  
 933 Sigrid Lehuta, Stéphanie Mahévas, David Makowsky, Hervé Monod, Benjamin Poussin, Eric  
 934 Ramat, Hervé Richard, Lauriane Rouan, Jean-Christophe Soulié, and Juhui Wang. 2013.



- 935 *Sensitivity analysis and model exploration: application to natural and environmental sciences*  
 936 *(Analyse de sensibilité et exploration de modèles: application aux sciences de la nature et de*  
 937 *l'environnement)*. Editions Quae. <http://site.ebrary.com/lib/uqat/Doc?id=10825807>.
- 938 Fernández-Pato, Javier, Daniel Caviedes-Voullième, and Pilar García-Navarro. 2016. 'Rainfall/Runoff  
 939 Simulation with 2D Full Shallow Water Equations: Sensitivity Analysis and Calibration of  
 940 Infiltration Parameters'. *Journal of Hydrology* 536 (May): 496–513.  
 941 <https://doi.org/10.1016/j.jhydrol.2016.03.021>.
- 942 Ferrant, Sylvain, François Oehler, Patrick Durand, Laurent Ruiz, Jordy Salmon-Monviola, Eric Justes,  
 943 Philippe Dugast, Anne Probst, Jean-Luc Probst, and José-Miguel Sanchez-Perez. 2011.  
 944 'Understanding Nitrogen Transfer Dynamics in a Small Agricultural Catchment: Comparison of  
 945 a Distributed (TNT2) and a Semi Distributed (SWAT) Modeling Approaches'. *Journal of*  
 946 *Hydrology* 406 (1–2): 1–15. <https://doi.org/10.1016/j.jhydrol.2011.05.026>.
- 947 Gaudou, Benoit, Christophe Sibertin-Blanc, Olivier Therond, Frédéric Amblard, Yves Auda, Jean-  
 948 Paul Arcangeli, Maud Balestrat, Charron, Marie-Hélène, Gondet, Etienne, Hong, Yi, Lardy,  
 949 Romain, Louail, Thomas, Mayor, Eunat, Panzoli, David, Sauvage, Sabine, Sánchez Pérez, José,  
 950 Taillandier, Patrick, Nguyen, Van, Vavasseur, Maroussia and Mazzega, Pierre. 2016. 'The  
 951 MAELIA Multi-Agent Platform for Integrated Assessment of Low-Water Management Issues'.  
 952 *MABS 2013-14th International Workshop on Multi-Agent-Based Simulation*, May.
- 953 Grayson, Rodger B., Ian D. Moore, and Thomas A. McMahon. 1992. 'Physically Based Hydrologic  
 954 Modeling: 2. Is the Concept Realistic?' *Water Resources Research* 28 (10): 2659–66.  
 955 <https://doi.org/10.1029/92WR01259>.
- 956 Gumiere, Silvio Jose, Damien Raclot, Bruno Cheviron, Gregory Davy, Xavier Louchart, Jean-  
 957 Christophe Fabre, Roger Moussa, and Yves Le Bissonnais. 2011. 'MHYDAS-Erosion: A  
 958 Distributed Single-Storm Water Erosion Model for Agricultural Catchments'. *Hydrological*  
 959 *Processes* 25 (11): 1717–28. <https://doi.org/10.1002/hyp.7931>.

- 960 Güntner, Andreas, Maarten S. Krol, José Carlos De Araújo, and Axel Bronstert. 2004. 'Simple Water  
961 Balance Modelling of Surface Reservoir Systems in a Large Data-Scarce Semiarid Region'.  
962 *Hydrological Sciences Journal* 49 (5): 901-18. <https://doi.org/10.1623/hysj.49.5.901.55139>.
- 963 Habets, Florence, Jérôme Molénat, Nadia Carluer, Olivier Douez, and Delphine Leenhardt. 2018. 'The  
964 Cumulative Impacts of Small Reservoirs on Hydrology: A Review'. *Science of The Total  
965 Environment* 643 (December): 850–67. <https://doi.org/10.1016/j.scitotenv.2018.06.188>.
- 966 Habets, Florence, Elodie Philippe, Eric Martin, Cervantes Hernández David, and Frédéric Leseur.  
967 2014. 'Small Farm Dams: Impact on River Flows and Sustainability in a Context of Climate  
968 Change'. *Hydrology and Earth System Sciences* 18 (10): 4207–22. [https://doi.org/10.5194/hess-  
969 18-4207-2014](https://doi.org/10.5194/hess-18-4207-2014).
- 970 Hallema, Dennis W., Roger Moussa, Patrick Andrieux, and Marc Voltz. 2013. 'Parameterization and  
971 Multi-Criteria Calibration of a Distributed Storm Flow Model Applied to a Mediterranean  
972 Agricultural Catchment'. *Hydrological Processes* 27 (10): 1379–98.  
973 <https://doi.org/10.1002/hyp.9268>.
- 974 Herman, Jonathan D., Joshua B. Kollat, Patrick M. Reed, and Thorsten Wagener. 2013. 'Technical  
975 Note: Method of Morris Effectively Reduces the Computational Demands of Global Sensitivity  
976 Analysis for Distributed Watershed Models'. *Hydrology and Earth System Sciences Discussions*  
977 10 (4): 4275–99. <https://doi.org/10.5194/hessd-10-4275-2013>.
- 978 Hermida, Lucía, Laura López, Andrés Merino, Claude Berthet, Eduardo García-Ortega, José Luis  
979 Sánchez, and Jean Dessens. 2015. 'Hailfall in Southwest France: Relationship with Precipitation,  
980 Trends and Wavelet Analysis'. *Atmospheric Research* 156: 174–88.  
981 <https://doi.org/10.1016/j.atmosres.2015.01.005>.
- 982 Hoogeveen, Jippe, Jean-Marc Faurès, Livia Peiser, Jacob Burke, and Nick van de Giesen. 2015.  
983 'GlobWat – a Global Water Balance Model to Assess Water Use in Irrigated Agriculture'.

- 984 *Hydrology and Earth System Sciences* 19 (9): 3829–44. [https://doi.org/10.5194/hess-19-3829-](https://doi.org/10.5194/hess-19-3829-2015)  
985 [2015](https://doi.org/10.5194/hess-19-3829-2015).
- 986 Hughes, Denis A., and Sukhamani K. Mantel. 2010. ‘Estimating the Uncertainty in Simulating the  
987 Impacts of Small Farm Dams on Streamflow Regimes in South Africa’. *Hydrological Sciences*  
988 *Journal* 55 (4): 578–92. <https://doi.org/10.1080/02626667.2010.484903>.
- 989 IGN. 2017. ‘DEM RGE ALTI 5m’. Database. France. [https://www.data.gouv.fr/fr/datasets/registre-](https://www.data.gouv.fr/fr/datasets/registre-parcellaire-graphique-rpg-contours-des-parcelles-et-ilots-cultureaux-et-leur-groupe-de-cultures-majoritaire/#)  
990 [parcellaire-graphique-rpg-contours-des-parcelles-et-ilots-cultureaux-et-leur-groupe-de-cultures-](https://www.data.gouv.fr/fr/datasets/registre-parcellaire-graphique-rpg-contours-des-parcelles-et-ilots-cultureaux-et-leur-groupe-de-cultures-majoritaire/#)  
991 [majoritaire/#](https://www.data.gouv.fr/fr/datasets/registre-parcellaire-graphique-rpg-contours-des-parcelles-et-ilots-cultureaux-et-leur-groupe-de-cultures-majoritaire/#).
- 992 IGN. 2016. ‘Digital aerial photography (Prises de vues aériennes dématérialisée)’. Photographs.  
993 France. <https://www.data.gouv.fr/fr/datasets/prises-de-vue-aeriennes-dematerialisees-de-lign/>.
- 994 IGN. 2015. ‘Land Parcel Identification System (Registre Parcellaire Graphique, RPG)’. Database.  
995 France. [https://www.data.gouv.fr/fr/datasets/registre-parcellaire-graphique-rpg-contours-des-](https://www.data.gouv.fr/fr/datasets/registre-parcellaire-graphique-rpg-contours-des-parcelles-et-ilots-cultureaux-et-leur-groupe-de-cultures-majoritaire/#)  
996 [parcelles-et-ilots-cultureaux-et-leur-groupe-de-cultures-majoritaire/#](https://www.data.gouv.fr/fr/datasets/registre-parcellaire-graphique-rpg-contours-des-parcelles-et-ilots-cultureaux-et-leur-groupe-de-cultures-majoritaire/#).
- 997 Jordan, David. 1990. ‘Implementation Benefits of C++ Language Mechanisms’. *Communications of*  
998 *the ACM* 33 (9): 61–64. <https://doi.org/10.1145/83880.84460>.
- 999 Kirchner, James W. 2009. ‘Catchments as Simple Dynamical Systems: Catchment Characterization,  
1000 Rainfall-Runoff Modeling, and Doing Hydrology Backward’. *Water Resources Research* 45 (2).  
1001 <https://doi.org/10.1029/2008WR006912>.
- 1002 Kollet, Stefan J., and Reed M. Maxwell. 2008. ‘Capturing the Influence of Groundwater Dynamics on  
1003 Land Surface Processes Using an Integrated, Distributed Watershed Model’. *Water Resources*  
1004 *Research* 44 (2). <https://doi.org/10.1029/2007WR006004>.
- 1005 Lee, Yooyoung, James J. Filliben, Ross J. Micheals, and P. Jonathon Phillips. 2013. ‘Sensitivity  
1006 Analysis for Biometric Systems: A Methodology Based on Orthogonal Experiment Designs’.

- 1007 *Computer Vision and Image Understanding* 117 (5): 532–50.  
 1008 <https://doi.org/10.1016/j.cviu.2013.01.003>.
- 1009 Leenhardt, Delphine, Olivier Therond, Marie-Odile Cordier, Chantal Gascuel-Odoux, Arnaud  
 1010 Reynaud, Patrick Durand, Jacques-Eric Bergez, Lucie Clavel, Véronique Masson, and Pierre  
 1011 Moreau. 2012. ‘A Generic Framework for Scenario Exercises Using Models Applied to Water-  
 1012 Resource Management’. *Environmental Modelling & Software* 37 (November): 125–33.  
 1013 <https://doi.org/10.1016/j.envsoft.2012.03.010>.
- 1014 Leenhardt D., Angevin F., Biarnes A., Colbach N., Mignolet C., 2010. Describing and locating  
 1015 cropping systems on a regional scale. A review. *Agronomy for Sustainable Development* 30 :  
 1016 131–138, DOI: 10.1051/agro/2009002. <http://dx.doi.org/10.1051/agro/2009002>
- 1017 Leenhardt D., Therond O., Mignolet C., 2020. Chapitre 9. Décrire les systèmes de culture pour la  
 1018 gestion intégrée des ressources en eau. In : Leenhardt D., Voltz M., Barreteau O. (Eds). *L'eau en*  
 1019 *milieu agricole. Outils et méthodes pour une gestion intégrée et territoriale. Collection Synthèses,*  
 1020 *Éditions Quæ, 2020, ISBN 978-2-7592-3123-2. p.141-152*
- 1021
- 1022 LEMA. 2006. *French Law on Water and Aquatic Environment (Loi sur l'Eau et les Milieux*  
 1023 *Aquatiques, LEMA). Environmental Code. Vol. 214–18, Law n°2006-1772.*  
 1024 <https://www.legifrance.gouv.fr/jorf/id/JORFTEXT000000649171>.
- 1025 Lewis, David C., and Robert H. Burgy. 1964. ‘The Relationship between Oak Tree Roots and  
 1026 Groundwater in Fractured Rock as Determined by Tritium Tracing’. *Journal of Geophysical*  
 1027 *Research* 69 (12): 2579–88. <https://doi.org/10.1029/JZ069i012p02579>.
- 1028 Lowe, L., Nathan, R., and Morden, R. (2005). “Assessing the impact of farm dams on streamflows,  
 1029 Part II: Regional characterisation.” *Aust. J. Water Resour.*, 9(1), 13–26

- 1030 Lowe, L.D., J.A. Webb, R.J. Nathan, T. Etchells, and H.M. Malano (2009), Evaporation from water  
1031 supply reservoirs: An assessment of uncertainty, *J. Hydrol.*, 376(1-2), 261–274,  
1032 doi:10.1016/j.jhydrol.2009.07.037.
- 1033 Malakoff David, Andrew Sugden, 2020, Dry times, *Science*, Vol. 368, Issue 6488, pp. 254-255, DOI:  
1034 10.1126/science.abc0396
- 1035 Maharjan, Ganga Ram, Youn Shik Park, Nam Won Kim, Dong Seok Shin, Jae Wan Choi, Geun Woo  
1036 Hyun, Ji-Hong Jeon, Yong Sik Ok, and Kyoung Jae Lim. 2013. ‘Evaluation of SWAT Sub-Daily  
1037 Runoff Estimation at Small Agricultural Watershed in Korea’. *Frontiers of Environmental  
1038 Science & Engineering* 7 (1): 109–19. <https://doi.org/10.1007/s11783-012-0418-7>.
- 1039 McJannet, D. L., F. J. Cook, and S. Burn (2013), Comparison of techniques for estimating evaporation  
1040 from an irrigation water storage, *Water Resour. Res.*, 49, 1415–1428, doi:10.1002/wrcr.20125
- 1041 Mishra, Surendra Kumar, Jaivir V. Tyagi, and Vijay P. Singh. 2003. ‘Comparison of Infiltration  
1042 Models’. *Hydrological Processes* 17 (13): 2629–52. <https://doi.org/10.1002/hyp.1257>.
- 1043 Moreno, Gerardo, José J. Obrador, Elena Cubera, and Christian Dupraz. 2005. ‘Fine Root Distribution  
1044 in Dehesas of Central-Western Spain’. *Plant and Soil* 277 (1–2): 153–62.  
1045 <https://doi.org/10.1007/s11104-005-6805-0>.
- 1046 Moriasi, Daniel N., Margaret W. Gitau, Naresh Pai, and Prasad Daggupati. 2015. ‘Hydrologic and  
1047 Water Quality Models: Performance Measures and Evaluation Criteria’. *Transactions of the  
1048 ASABE* 58 (6): 1763–85. <https://doi.org/10.13031/trans.58.10715>.
- 1049 Moussa, Roger, Nanée Chahinian, and Claude Bocquillon. 2007. ‘Distributed Hydrological Modelling  
1050 of a Mediterranean Mountainous Catchment – Model Construction and Multi-Site Validation’.  
1051 *Journal of Hydrology* 337 (1–2): 35–51. <https://doi.org/10.1016/j.jhydrol.2007.01.028>.

- 1052 Moussa, Roger, Marc Voltz, and Patrick Andrieux. 2002. 'Effects of the Spatial Organization of  
1053 Agricultural Management on the Hydrological Behaviour of a Farmed Catchment during Flood  
1054 Events'. *Hydrological Processes* 16 (2): 393–412. <https://doi.org/10.1002/hyp.333>.
- 1055 MTES. 2012. 'CORINE Land Cover'. Database. France. [https://www.data.gouv.fr/fr/datasets/corine-](https://www.data.gouv.fr/fr/datasets/corine-land-cover-occupation-des-sols-en-france/)  
1056 [land-cover-occupation-des-sols-en-france/](https://www.data.gouv.fr/fr/datasets/corine-land-cover-occupation-des-sols-en-france/).
- 1057 Murgue, Clément, Romain Lardy, Maroussia Vavasseur, Delphine Leenhardt, and Olivier Therond.  
1058 2014. 'Fine Spatio-Temporal Simulation of Cropping and Farming Systems Effects on Irrigation  
1059 Withdrawal Dynamics within a River Basin'. In *International Environmental Modelling and  
1060 Software Society (IEMSs): Agro-Ecosystem Modeling for Spatial Solutions to Watershed  
1061 Conundrums*, 4:1817–24. San Diego, CA, USA. <https://hal.inrae.fr/hal-02741968/document>.
- 1062 Murgue C., Therond O., Leenhardt D., 2016. Hybridizing local and generic information to model  
1063 cropping system spatial distribution in an agricultural landscape. *Land Use Policy*, 54, 339-354.  
1064 <http://dx.doi.org/10.1016/j.landusepol.2016.02.020>
- 1065 Nash, James E., and John V. Sutcliffe. 1970. 'River Flow Forecasting through Conceptual Models Part  
1066 I — A Discussion of Principles'. *Journal of Hydrology* 10 (3): 282–90.  
1067 [https://doi.org/10.1016/0022-1694\(70\)90255-6](https://doi.org/10.1016/0022-1694(70)90255-6).
- 1068 Nathan, Rory, Phillip Jordan, and Robert Morden. 2005. 'Assessing the Impact of Farm Dams on  
1069 Streamflows, Part I: Development of Simulation Tools'. *Australasian Journal of Water  
1070 Resources* 9 (1): 1–12. <https://doi.org/10.1080/13241583.2005.11465259>.
- 1071 Neitsch, Susan L., Jeff G. Arnold, James R. Kiriny, and Jimmy R. Williams. 2011. *Soil & Water  
1072 Assessment Tool - Theoretical Documentation*. Version 2009. Texas Water Resources Institute  
1073 Technical Report 406. Texas, USA: Texas A&M University System.

- 1074 Ogilvie, A., Belaud, G., Massuel, S., Mulligan, M., Le Goulven, P., Calvez, R., 2016. Assessing  
1075 Floods and Droughts in Ungauged Small Reservoirs with Long-Term Landsat Imagery.  
1076 *Geosciences* 6, 42. <https://doi.org/10.3390/geosciences6040042>
- 1077 Oudin, Ludovic, Vazken Andréassian, Thibault Mathevet, Charles Perrin, and Claude Michel. 2006.  
1078 ‘Dynamic Averaging of Rainfall-Runoff Model Simulations from Complementary Model  
1079 Parameterizations’. *Water Resources Research* 42 (7). <https://doi.org/10.1029/2005WR004636>.
- 1080 Party, Jean-Paul, Nicolas Muller, Quentin Vauthier, Laurent Rigou, Benoît Toutain, Sébastien  
1081 Lehmann, Bertrand Laroche, and Maritxu Guiresse. 2016. ‘Regional Pedological Databank of  
1082 Midi-Pyrénées : Gers Department (Référentiel Régional Pédologique de Midi-Pyrénées :  
1083 Département du Gers)’. CNRS/EcoLab. <https://doi.org/10.6096/70324>.
- 1084 Perrin, Jérôme, Sylvain Ferrant, Sylvain Massuel, Benoit Dewandel, Jean-Christophe Maréchal,  
1085 Stéphanie Aulong, and Shakeel Ahmed. 2012. ‘Assessing Water Availability in a Semi-Arid  
1086 Watershed of Southern India Using a Semi-Distributed Model’. *Journal of Hydrology* 460–461  
1087 (August): 143–55. <https://doi.org/10.1016/j.jhydrol.2012.07.002>.
- 1088 Potter, Kenneth W. 2006. ‘Small-Scale, Spatially Distributed Water Management Practices:  
1089 Implications for Research in the Hydrologic Sciences’. *Water Resources Research* 42 (3).  
1090 <https://doi.org/10.1029/2005WR004295>.
- 1091 Puissant, Anne, Arnaud Sellé, Nicolas Baghdadi, Vincent Thierion, Arnaud Le Bris, and Jean-Louis  
1092 Roujean. 2019. ‘The “Urban” Component of the French Land Data and Services Centre  
1093 (THEIA)’. In 2019, *Joint Urban Remote Sensing Event (JURSE)*, 1–4. Vannes, France: IEEE.  
1094 <https://ieeexplore.ieee.org/abstract/document/8808998>.
- 1095 Pushpalatha, Raji, Charles Perrin, Nicolas Le Moine, and Vazken Andréassian. 2012. ‘A Review of  
1096 Efficiency Criteria Suitable for Evaluating Low-Flow Simulations’. *Journal of Hydrology* 420–  
1097 421 (February): 171–82. <https://doi.org/10.1016/j.jhydrol.2011.11.055>.

- 1098 Quintana-Seguí, Pere, Patrick Le Moigne, Yves Durand, Eric Martin, Florence Habets, Martine  
 1099 Baillon, Claire Canellas, Laurent Franchisteguy, and Sophie Morel. 2008. ‘Analysis of Near-  
 1100 Surface Atmospheric Variables: Validation of the SAFRAN Analysis over France’. *Journal of*  
 1101 *Applied Meteorology and Climatology* 47 (1): 92–107.  
 1102 <https://doi.org/10.1175/2007JAMC1636.1>.
- 1103 Rahman, Mohammad M., Minjiao Lu, and Khin H. Kyi. 2016. ‘Seasonality of Hydrological Model  
 1104 Spin-up Time: A Case Study Using the Xinanjiang Model’. *Hydrology and Earth System*  
 1105 *Sciences Discussions*, July, 1–22. <https://doi.org/10.5194/hess-2016-316>.
- 1106 Rizzo D., Therond O., Lardy R., Murgue C., Leenhardt D., 2019. A rapid, spatially explicit approach  
 1107 to describe cropping systems dynamics at the regional scale. *Agricultural Systems*, 173: 491-503,  
 1108 ISSN 0308-521X, <https://doi.org/10.1016/j.agsy.2019.04.003>
- 1109 Rosa, Lorenzo, Davide Danilo Chiarelli, Matteo Sangiorgio, Areidy Aracely Beltran-Peña, Maria  
 1110 Cristina Rulli, Paolo D’Odorico, and Inez Fung. 2020a. ‘Potential for Sustainable Irrigation  
 1111 Expansion in a 3 °C Warmer Climate’. *Proceedings of the National Academy of Sciences* 117  
 1112 (47): 29526–34. <https://doi.org/10.1073/pnas.2017796117>.
- 1113 Rosa, Lorenzo, Davide Danilo Chiarelli, Maria Cristina Rulli, Jampel Dell’Angelo, and Paolo  
 1114 D’Odorico. 2020b. ‘Global Agricultural Economic Water Scarcity’. *Science Advances* 6 (18): 1–  
 1115 10. <https://doi.org/10.1126/sciadv.aaz6031>.
- 1116 Rousseau, A.N., S. Savary, D.W. Hallema, S.J. Gumiere, E. Foulon. 2013. the effects of agricultural  
 1117 BMPs on sediments, nutrients and water quality of the Beaurivage River watershed  
 1118 (Quebec,Canada) *Canadian Water Resources Journal*, 38(2): 99-120.  
 1119 DOI:10.1080/07011784.2013.780792
- 1120 Sheffield, Justin, and Eric F. Wood. 2008. ‘Projected Changes in Drought Occurrence under Future  
 1121 Global Warming from Multi-Model, Multi-Scenario, IPCC AR4 Simulations’. *Climate Dynamics*  
 1122 31 (1): 79–105. <https://doi.org/10.1007/s00382-007-0340-z>.



- 1123 Skaggs, Richard W., Marlón A. Brevé, and James W. Gilliam. 1994. 'Hydrologic and Water Quality  
 1124 Impacts of Agricultural Drainage\*'. *Critical Reviews in Environmental Science and Technology*  
 1125 24 (1): 1–32. <https://doi.org/10.1080/10643389409388459>.
- 1126 Spinoni, Jonathan, Gustavo Naumann, Hugo Carrao, Paulo Barbosa, and Jürgen Vogt. 2014. 'World  
 1127 Drought Frequency, Duration, and Severity for 1951–2010'. *International Journal of*  
 1128 *Climatology* 34 (8): 2792–2804. <https://doi.org/10.1002/joc.3875>.
- 1129 Stafford, John V., Bruce Ambler, Murray R. Lark, and John A. Catt. 1996. 'Mapping and Interpreting  
 1130 the Yield Variation in Cereal Crops'. *Computers and Electronics in Agriculture* 14 (2–3): 101–  
 1131 19. [https://doi.org/10.1016/0168-1699\(95\)00042-9](https://doi.org/10.1016/0168-1699(95)00042-9).
- 1132 Tarboton, Kenneth C., and Roland E. Schulze. 1991. 'The ACRU Modelling System for Large  
 1133 Catchment Water Resources Management'. In *Hydrology for the Water Management of Large*  
 1134 *River Basins. International Symposium. General Assembly of the International Union of Geodesy*  
 1135 *and Geophysics (20)*, 219–32. IAHS-AISH Publication. United Kingdom: International  
 1136 Association of Hydrological Sciences, Wallingford.  
 1137 [http://hydrologie.org/redbooks/a201/iahs\\_201\\_0219.pdf](http://hydrologie.org/redbooks/a201/iahs_201_0219.pdf).
- 1138 Therond, Olivier, Christophe Sibertin-Blanc, Romain Lardy, Benoît Gaudou, Maud Balestrat, Yi  
 1139 Hong, Thomas Louail, Van Bai Nguyen, David Panzoli, José-Miguel Sánchez-Pérez, Sabine  
 1140 Sauvage, Patrick Taillandier, Maroussia Vavasseur, Pierre Mazzega. 2014. 'Integrated Modelling  
 1141 of Social-Ecological Systems: The MAELIA High-Resolution Multi-Agent Platform to Deal  
 1142 with Water Scarcity Problems'. In *7. International Congress on Environmental Modelling and*  
 1143 *Software (IEMSs 2014)*, 2386 p. Proceedings of the 7th International Congress on Environmental  
 1144 Modelling and Software, June 15–19, San Diego, California, USA. San Diego, Californie, United  
 1145 States: International Environmental Modelling and Software Society (iEMSs).  
 1146 <https://hal.inrae.fr/hal-02742949>.

- 1147 Therond, Olivier, and Jean Villerd. 2020. 'Modelling of socio-Agro-Ecological system for Landscape  
1148 Integrated Assessment'. Documentation. Documentation plateforme Maelia. January 2020.  
1149 <http://maelia-platform.inra.fr/accueil/contributeurs/>. (accessed 5.6.20).
- 1150 Vörösmarty, Charles J., Pamela Green, Joseph Salisbury, and Richard B. Lammers. 2000. 'Global  
1151 Water Resources: Vulnerability from Climate Change and Population Growth'. *Science* 289  
1152 (5477): 284–88. <https://doi.org/10.1126/science.289.5477.284>.
- 1153 Wisser, Dominik, Steve Frohking, Ellen M. Douglas, Balazs M. Fekete, Andreas H. Schumann, and  
1154 Charles J. Vörösmarty. 2010. 'The Significance of Local Water Resources Captured in Small  
1155 Reservoirs for Crop Production – A Global-Scale Analysis'. *Journal of Hydrology* 384 (3–4):  
1156 264–75. <https://doi.org/10.1016/j.jhydrol.2009.07.032>.
- 1157 Zhang, Chi, Yong Peng, Jinggang Chu, Christine A. Shoemaker, and Aijing Zhang. 2012. 'Integrated  
1158 Hydrological Modelling of Small- and Medium-Sized Water Storages with Application to the  
1159 Upper Fengman Reservoir Basin of China'. *Hydrology and Earth System Sciences* 16 (11):  
1160 4033–47. <https://doi.org/10.5194/hess-16-4033-2012>.  
1161  
1162

## 1163 **Appendix A: Simulation rules used for farmer management decisions**

1164 The farmer management decisions considered in the model include tillage, sowing, harvest and  
1165 irrigation. The decision rules adopted to simulate these technical operations are described below. The  
1166 variables employed as indicators are mentioned between brackets.

1167 • A tillage day occurs during the tillage period (temporal window) according to the soil type,  
1168 when the soil water content is favourable, i.e., this depends on the weather conditions (antecedent  
1169 cumulative rainfall) and soil conditions (soil water content);

1170 • A sowing day may occur on the first day of the simulation or after the harvesting period,  
1171 which depends on the weather conditions (antecedent cumulative rainfall and minimal temperature),  
1172 possible sowing period (temporal window) according to the crop type and precocity class and soil  
1173 conditions (soil water content);

1174 • A harvesting day is simulated either when the crop is mature (crop development stage) or  
1175 before poor soil and weather conditions occur (antecedent cumulative rainfall and soil water content),  
1176 which could result in soil damage;

1177 • Depending on the development of the crop and the weather conditions (previous rainfall and  
1178 rainfall forecasts), the water demand for irrigation may be zero or have a non-zero fixed value. This  
1179 fixed value depends on the crop, the soil and the irrigation equipment. It is a model parameter (e.g., 30  
1180 mm for maize in the Gelon catchment application). The volume of water actually withdrawn and  
1181 delivered to the cultivated field is conditioned by the availability of the water resource (see section  
1182 1.4.2). The farmer's water demand is calculated at a time step depending on the farmer's equipment  
1183 constraints. The time step is a model parameter (e.g., 6 or 7 days in the Gelon catchment application  
1184 depending on the field).

1185

1186 **Appendix B: Description of the MHYDAS-Small-Reservoirs simulator**

1187 Number (Nb.), name, model component, spatial unit type and main simulated variables of every  
 1188 simulator constituting MHYDAS-Small-Reservoirs. The model component refers to the integrated  
 1189 model component, namely, hydrology (Hydrol.), crop growth (Crop) or crop and agricultural water  
 1190 management (Water Manag.).

Nb.	Name of the simulator	Model component	Unit type	Main simulated variables
1	water.atm-surf.evapotranspiration-su.files	Hydrol. and Crop	SU	Reference evapotranspiration
2	water.atm-surf.evaporation-re.files	Hydrol.	RE	Reference evaporation
3	water.atm-surf.rain-su.files	Hydrol.	SU	Rainfall
4	water.atm-surf.rain-re.files	Hydrol.	RE	Rainfall
5	energy.atm-surf.T.temperature	Crop	SU	Mean air temperature
6	energy.atm-surf.T.temperature-min	Crop	SU	Minimum air temperature
7	water.surf.ecological-flow-rs-re.mean-annual-discharge	Water Manag.	RE	Ecological flow
8	crop.surf.practices-su.decision-Murgue	Crop and Water Manag.	SU	Farmer management decisions (sowing day, tillage day, harvesting day, irrigation day, and irrigation water demand)
9	crop.surf.practices-su.application-Murgue	Crop and Water Manag.	SU	Application of Farmer management decisions (sowing day, tillage day, harvesting day, irrigation day, and irrigation water demand)
10	water.surf-sz.abstraction-priority-wp.decision-order	Water Manag.	WP*	Priority order for irrigation

11	water.surf.withdrawal-irrigation- wp.prorata-water-demand	Crop and Water Manag.	WP*	Available water for irrigation Total irrigation water demand Water withdrawal Irrigation
12	water-soil-crop.surf-uz.runoff- cropsoilwaterdynamics-transfer-su- storage-non-connected-re.Horton- Hayami-AqYield-water-balance	Crop and Hydrol.	SU	Infiltration Crop growth Evapotranspiration Percolation Surface runoff Soil water content Crop water requirement
			RE	Overflow Water storage Evaporation
13	water-soil.surf-uz.percolation- evapotranspiration-su.soil-swat	Hydrol.	SU	Evapotranspiration Percolation
14	water.surf-sz.storage-baseflow- gu.storage-discharge-function	Hydrol.	GU	Water storage Discharge and baseflow
15	water.surf.transfer-rs-storage- connected-re.hayami-water-balance	Hydrol.	RS	Stream runoff
			RE	Overflow Water storage Evaporation
16	water.surf.variable-surface- re.bathymetric-relation	Hydrol.	RE	Water surface area

1191 \* WP (withdrawal point) corresponds to a water resource (RS or RE) dedicated to irrigation

1192

1193 **Appendix C: Main parameters of the MHYDAS-Small-Reservoirs model**

1194 List of the main MHYDAS-Small-Reservoirs model parameters given by spatial unit type. For each  
 1195 parameter, the spatial unit type, the model relying on it, a description of the parameter with values of  
 1196 the non-distributed parameters and the origin database are listed. Bold and italicised numbers indicate  
 1197 the number of the simulator, as referenced in Appendix B, that relies on that parameter.

<i>Unit type</i>	<i>Model component</i>	<i>Parameters</i>	<i>Data sources used in the Gélon application</i>
SU (agricultural)	Crop	Crop type ( <b>8</b> , <b>12</b> )	Land Parcel Identification System of 2015 (IGN, 2015)
		Crop growth potential, root growth coefficient, evaporation coefficient and sum of the growing degree days at the maturity and flowering stages ( the complete list of AqYield parameters can be found on the Maelia website <a href="http://maelia-platform.inra.fr/donnees/donnees-agricoles/liste-des-cultures/">http://maelia- platform.inra.fr/donnee s/donnees- agricoles/liste-des- cultures/</a> ) ( <b>12</b> )	Table of crop cultivar characteristics provided by breeders and AqYield calibration (Constantin et al., 2015)
SU (non-agricultural)	Hydrol.	Type of land use ( <b>12</b> , <b>13</b> )	Land use inventory of 2012 (MTES, 2012)

		Grassland root depth: 0.80 m ( <b>I3</b> )	Moreno et al. (2005)
		Forest root depth: the maximum soil depth ( <b>I3</b> )	Lewis & Burgy (1964), Algayer et al. (2020)
<b>SU</b>	Crop and Water Manag.	(Agricultural SUs) Technical itinerary according to the type of crop, soil and irrigation equipment ( <b>8</b> ); irrigation equipment ( <b>8</b> )	Gaudou et al. (2016), Murgue et al. (2014), Therond and Villerd (2020), field surveys
<b>SU</b>	Hydrol.	Soil minimum infiltration capacity coefficient ( <b>I2</b> ); Soil maximum infiltration capacity coefficient ( <b>I2</b> ); and shape coefficient ( <b>I2</b> )	Mishra et al. (2003), Fernández-Pato et al. (2016), sensitivity analysis
		Soil maximum infiltration capacity, bulk density, clay rate, potential maximal available water content, and thickness ( <b>I2, I3</b> )	Regional Pedological Databank (Party et al., 2016)
<b>RS and SU</b>	Hydrol.	Manning ( $\text{m}\cdot\text{s}^{-1}$ ): 0.05 (SU); 0.10 (RS) ( <b>I2, I5</b> )	Chow (1959)
		Celerity ( $\text{m}^2\cdot\text{s}^{-1}$ ): 0.045 (SU); 0.49 (RS) ( <b>I2, I5</b> ); diffusivity ( $\text{m}\cdot\text{s}^{-1}$ ): 500	Moussa et al. (2002)

		(SU and RS) ( <i>12, 15</i> ); iteration number in Hayami kernel calculations: 100 ( <i>12, 15</i> )	
<b>RE</b>	Crop and Water Manag.	Irrigated plots ( <i>10</i> )	BD CACG-OUGC-DDT, completed by field surveys
<b>RE</b>	Hydrol. and Water Manag.	Evaporation coefficient (0.6) ( <i>2</i> )	Neitsch et al. (2011)
		Dead volume of the reservoir: 0.25 of the total capacity ( <i>11</i> )	Therond and Villerd (2020)
		Minimum flow: 10% of the interannual flow ( <i>7</i> )	LEMA (2006)
<b>GU</b>	Hydrol.	Reference flow ( $\text{m}^2 \cdot \text{s}^{-1}$ ): $5.365 \cdot 10^{-8}$ ( <i>14</i> ); divisor parameter (0.05) ( <i>14</i> ); exponential parameter (5.66) ( <i>14</i> )	Flow recession curve analysis

1198